A temperature-regulated circuit for feeding behavior

Shaowen Qian (✉ qianshaowen1110@163.com)
Army Medical University
Sumei Yan
Army Medical University
Ruiqi Pang
Army Medical University
Jing Zhang
Department of Radiation Oncology, Tianjin Medical University Cancer Institute and Hospital, National Clinical Research Center for Cancer
Kai Liu
Jinan Military General Hospital
Zhiyue Shi
Army Medical University
Zhaoqun Wang
Army Medical University
Chen Penghui
Army Medical University
Yanjie Zhang
Army Medical University
Tiantian Luo Luo
Army Medical University
Xianli Hu
Army Medical University
Ying Xiong
Third Military Medical University
Yi Zhou
Army Medical University https://orcid.org/0000-0002-2623-8960

Article

Keywords: feeding behavior, ambient temperature, medial preoptic area, arcuate nucleus, paraventricular hypothalamic nucleus

Posted Date: October 1st, 2021

DOI: https://doi.org/10.21203/rs.3.rs-916525/v1

Version of Record: A version of this preprint was published at Nature Communications on July 22nd, 2022. See the published version at https://doi.org/10.1038/s41467-022-31917-w.

Abstract

Both rodents and primates have evolved to orchestrate food intake to maintain thermal homeostasis in coping with ambient temperature challenges. However, the mechanisms underlying temperature-coordinated feeding behavior are rarely reported. Here we found that a non-canonical feeding center, the anteroventral and periventricular portions of medial preoptic area (apMPOA) responded to altered dietary states. Two neighboring but distinct apMPOA neurons mediated feeding in receiving anatomical inputs from external and dorsal subnuclei of lateral parabrachial nucleus (LPB). While both populations are glutamatergic, the arcuate nucleus (ARC)-projecting neurons in apMPOA can sense low temperature and promote food intake. The other type, the paraventricular hypothalamic nucleus (PVH)-projecting neurons in apMPOA are primarily sensitive to high temperature and suppress food intake. Cutting off both pathways can eliminate the temperature-dependence of feeding. Further projection-specific RNA sequencing identified that the two neuronal populations were molecularly marked by galanin receptor and apelin receptor. These findings reveal an unrecognized cell populations and circuits of apMPOA that orchestrates feeding behavior against thermal challenges.

Introduction

Feeding behavior is regulated by multiple hard-wired neural circuits that underlie diverse internal homeostatic factors and external environmental factors [1-5]. Ambient temperature, as a pivotal homeostatic-related environmental factor, intimately orchestrate feeding behavior [5-8]. To maintain homeostasis for survival, both rodents and primates have evolved to optimally orchestrate food intake in sensing ambient thermal challenges [9-13]. A long-standing theory for feeding behavior proposes a “thermostatic” mechanism, in which food intake acts as a mechanism of thermoregulation to maintain proper energy intake [9]. Under low ambient temperature, the higher demand for heat production forces body to further increase energy intake, which is manifested as a promoted feeding. In the instances of extremely hot environments, the lower thermal demand and higher dissipation load preferentially suppress food intake, overriding the dietary state [9,14,15]. However, the neural mechanisms underlying the ambient temperature-coordinated feeding behavior are rarely reported.

The neuronal populations in medial preoptic area (MPOA) have been identified be responsive to ambient temperature, including subpopulations of neurons that express leptin receptor [8,16], adenylate cyclase-activating peptide 1, brain-derived neurotrophic factor [17,18], and pyroglutamylated RFamide peptide [19]. Intermingled with thermosensory aspects, the activations of these neurons also resulted in changes in feeding behavior [8,16,19]. Local thermal manipulations (e.g., heating, cooling or lesions) on the MPOA in goats, rats or pigs would cause rapid feeding behavior or cessation, regardless of their original dietary states [14,15,20-24]. Genetically activating MPOA neurons even could cause mice to enter a state of hibernation or daily torpor, showing hypothermia and anorexia [18,19,25]. Pathologically, patients with hypothalamo-pituitary deficiency (e.g., craniopharyngioma, pituitary tumor) [26-28], as well as animals with lesions in the preoptic area and anterior hypothalamus (POA/AH) [15,21,29], usually exhibit abnormalities in

autonomic thermoregulation along with abnormal feeding behavior. Recently, anterograde labeling of MPOA neurons revealed dense projections to multiple appetite centers, such as the bed nucleus of the stria terminalis (BNST), arcuate nucleus (ARC), paraventricular hypothalamic nucleus (PVH), lateral hypothalamus (LH) [30,31]. It would be interesting to investigate whether thermosensitive MPOA neurons and their specific circuits exert neural regulations on appetite centers in coping with ambient thermal challenges.

To address these issues, we dissected the contribution of POA/AH to temperature-dependent feeding behavior. We found that among multiple thermosensitive subregions of the POA/AH, two populations of glutamatergic neurons in the anteroventral and periventricular portions of medial preoptic area (apMPOA) were responsive to altered dietary states, and orchestrated two distinct pathways to mediate feeding behavior in receiving thermal inputs from external and dorsal subnuclei of lateral parabrachial nucleus (LPB). The ARC-projecting neurons in apMPOA could sense low temperature, and promoted food intake. Whereas, the PVH-projecting neurons in apMPOA were primarily sensitive to high temperature and suppressed food intake. Further projection-specific RNA sequencing identified that the two neuronal populations were molecularly marked by galanin receptor and apelin receptor. Collectively, our results highlight a previously unrecognized cell populations and circuits of apMPOA that orchestrates feeding behavior in coping with ambient temperatures.

Results

1. **Glutamatergic neurons in the apMPOA respond to altered dietary states**

We first identified the behavioral pattern of temperature-dependent feeding behavior (Fig. 1a-b, Fig. S1). We observed that 2 hours of hot exposure reduced the food intake of the mice by 25.1%, whereas 2 hours of cold exposure increased food intake by 20.3% (Fig. 1b). The temperature-dependence of food intake persisted under longer thermal exposure of 12 hours (Fig. S1a). Ambient exposures did not result in loss of rectal temperature (Fig. S1b).

Next, we sought to determine whether central thermosensitive nuclei were involved in the phenotype of temperature-regulated feeding behavior. We deprived the mice of food for 12 hours and quantified C-Fos expression in the central thermosensitive nuclei. We observed substantial C-Fos expressions in the anteroventral periventricular portions of the medial preoptic area (apMPOA), including ventromedial POA (VMPO), anteroventral periventricular nucleus (AVPe), ventral median preoptic nucleus (MnPO), preoptic part of periventricular hypothalamic nucleus (PVpo) and anterior MPOA among multiple thermosensitive nuclei within the POA/AH, but not the lateral preoptic area (LPO), AH, medial preoptic nucleus (MPN), or lateral parabrachial nucleus (LPB) (Fig. 1c, and Fig. S2). Mice that were fed ad libitum or underwent refeeding for 2 hours after fasting showed no C-Fos expression in the apMPOA (Fig. 1d, 1e). To identify the cell types, we bred vGluT2-cre and GAD2-cre mice with Ai9 reporter mice, in which the vGluT2+ and GAD2+ neurons were labeled with tdTomato (Fig. 1g-h). The fasting-induced C-Fos in the apMPOA exhibited substantial colocalization with vGluT2+ neurons. Approximately 60% of C-Fos+ neurons

expressed vGluT2, whereas nearly 65% of vGluT2+ neurons expressed C-Fos (Fig. 1g, 1i, 1j). In the GAD2-cre::Ai9 mice, fasting-induced C-Fos exhibited minor overlap with the GAD2 (20% C-Fos+ neurons expressed GAD2) (Fig. 1h-j).

To further clarify the neuronal responses of apMPOA to dietary state, we injected activity-dependent GCaMP6s into the apMPOA of vGluT2-cre and GAD2-cre mice and installed an optical fiber above the apMPOA to record calcium signal during feeding (Fig. 1k). We found no significant calcium responses to the feeding in GAD2-cre mice during 15-min recordings (Fig. 1l-n). In contrast, vGluT2-cre mice showed a substantial signal decrease in 5 minutes after the onset of feeding, indicating that vGluT2+ neuron activity decreased substantially after the onset of feeding (Fig. 1m-n). Moreover, the decreased calcium response of glutamatergic apMPOA neurons did not occur upon sensory detection of food, or nonedible object (such as tearing paper), and did not recover after pausing feeding behavior (Movie S1). These findings indicated that glutamatergic apMPOA neurons, but not GABAergic neurons, responded to altered dietary states, such as hunger-activated response once overnight fasted, and satiety-inhibited response once refed.

2. **Optogenetic activation on glutamatergic apMPOA neurons modulates body temperature**

We next targeted the expression of channelrhodopsin-2 (ChR2) to glutamatergic and GABAergic apMPOA neurons to explore their regulatory roles in feeding (Fig. 2a-b). Remarkably, the food intake of apMPOA$^{vGluT2\text{-}ChR2}$ stimulated mice was significantly decreased by 89.1% compared with that of the mice receiving no opto-stimulation (Fig. 2c), while the light stimulation on apMPOA$^{GAD2\text{-}ChR2}$ neurons caused no significant change in food intake (Fig. 2c). Consistent with previous studies [8,32], as a thermosensitive and regulatory center, the opto-stimulation on apMPOA$^{vGluT2\text{-}ChR2}$ neurons, but not apMPOA$^{GAD2\text{-}ChR2}$ neurons, induced apparent autonomic thermoregulation of inhibited BAT thermogenesis, enhanced heat dissipation via tail vasodilation (Fig. 2d-e). Notably, we found that the activation of apMPOA$^{vGluT2\text{-}ChR2}$, but not apMPOA$^{GAD2\text{-}ChR2}$, led to a remarkable cold defensive behavior, nest building (Movies S2 and S3), which might indirectly affect food intake. The apMPOA comprises multiple cell types and downstream projections that mediate complex innate behaviors [30,33], and homeostatic regulatory processes [17,34]. Therefore, here we could not conclude that direct activation on the apMPOA$^{vGluT2\text{-}ChR2}$ suppressed food intake, which awaited further dissecting downstream regions of apMPOA$^{vGluT2\text{-}ChR2}$ neurons.

3. Optogenetic activations on terminal fibers of the apMPOA$^{vGluT2+}$ neurons in ARC and PVH orchestrate food intake

We next dissected the downstream targets of apMPOA$^{vGluT2+}$ neurons to explore the potential regulatory effect on food intake. We performed anterograde tracing by injecting AAV-DIO-hChR2-EYFP into the apMPOA of vGluT2-cre mice (Fig. 3a). Consistent with previous studies [30,31], and data from the Allen Brain Atlas (Experiment 113554719, http://connectivity.brain-map.org/), we found that apMPOA$^{vGluT2+}$ neurons exhibited widespread projections to multiple brain regions involved in feeding

behavior, including the BNST, LH, tuberal nucleus (TN), PVH, dorsomedial hypothalamic nucleus (DMH), ARC, paraventricular thalamic nucleus (PVT), basolateral and basomedial amygdala (BA), ventral tegmental area (VTA) and periaqueductal gray (PAG) (Fig. 3b, Fig. S3b). We quantified neurons directly under apMPOA$^{vGluT2+}$ axons that expressed hunger-induced C-Fos. The number of neurons expressing C-Fos was increased in several downstream regions, including PVH, ARC, LH, DMH, BNST, PAG (Fig. 3b), but not in the others, including PVT, TN, BA and VTA (Fig. S3b).

Among the downstream regions of apMPOA$^{vGluT2+}$ neurons, several were previously reported to be involved in regulating feeding behavior [35-38], raising the hypothesis that these apMPOA-projecting neural pathways are probably involved in temperature-regulating feeding behavior. We performed a systematic manipulation on each downstream region of apMPOA$^{vGluT2+}$ neurons (Fig. 3c, Fig. S3a). We discovered that optogenetic activation on apMPOA→ARC terminal fibers increased food intake by 56.8% (Fig. 3d). In contrast, terminal activation on the PVH reduced food intake by 78.1% (Fig. 3d). The regulatory effects on food intake of terminal activations on both ARC and PVH were robust under high and low ambient temperature (Fig. 3e-f), and did not cause changes in rectal temperature (Fig. S3i) or cold defensive behavior mentioned above. These findings indicated that glutamatergic apMPOA neurons could specifically orchestrate feeding behavior through downstream regions ARC/PVH. Additionally, terminal activation on the DMH reduced food intake by 84.5% (Fig. 3d). However, the mice exhibited apparent nest building, a cold defensive behavior, which may indirectly disturb feeding behavior (Fig. S3k-l, Movie S4). The DMH was previously reported to be involved in behavioral thermoregulation [39]. Therefore, the regulatory effect of the apMPOA→DMH pathway on feeding behavior awaits further verification. In the controls, light delivery to the apMPOA→ARC/PVH/DMH terminal fibers with YFP expression did not result in changes of food intake or rectal temperature (Fig. S3f-h, j). Additionally, terminal activations on the other downstream targets, including LH, BNST, PAG, PVT, TN, BA and VTA, had no effect on food intake or rectal temperature (Fig. S3c-e, i).

4. Genetic ablation and chemogenetic inhibition on the postsynaptic neurons of apMPOA to ARC/PVH pathways reversely modulates feeding behavior

Considering that optogenetic terminal activation might cause nonspecific antidromic stimulation of collateral targets, we next assessed the necessity of the apMPOA→ARC/PVH/DMH pathways for regulating feeding behavior by injecting AAV1-cre-GFP into the apMPOA and AAV-flex-taCasp3-TEVp into the ARC, PVH, and DMH (Fig. 4a). With this approach, the apMPOA-recipient postsynaptic neurons in the ARC, PVH, and DMH would be selectively ablated after expressing Caspase-3, but express fluorescent protein GFP and not be ablated in the controls without Caspase-3 (Fig. 4b, 4d, Fig. S4b). The ablation of apMPOA-recipient ARC neurons reduced food intake during normothermia by 32.9% (Fig. 4e). Reduced food intake was also observed during high and low ambient temperature (Fig. 4e). In contrast, the ablation of apMPOA-recipient PVH neurons increased food intake during normothermia by 62.3%, as well as high and low ambient temperature (Fig. 4c). The ablations of both pathways specifically mediate food intake, as they had no effects on rectal temperature (Fig. S4d-e). Regarding to the apMPOA→DMH

pathway, we selectively ablated apMPOA-recipient DMH neurons (Fig. S4b), and found that the ablation had no influence on food intake during normothermia (Fig. S4c). This indicated that the apMPOA→DMH pathway did not contribute to feeding regulation. Moreover, the ablation resulted in defective thermoregulation under rapid thermal challenge, since their rectal temperature fluctuated as ambient temperatures (Fig. S4f). The thermal imbalance might indirectly affect food intake during both high and low ambient temperature (Fig. S4c). These results indicated that the apMPOA→DMH pathway differs from the other two effector pathways, and may be primarily involved in autonomic and behavioral thermoregulation. Thus, a role of this pathway in the direct regulation on feeding behavior was excluded.

We also reversely manipulated the apMPOA circuits using chemogenetic inhibition on the apMPOA-recipient neurons in the ARC and PVH that express inhibitory designer receptor exclusively activated by designer drugs (DREADD-Gi), hM4Di, and be inhibited after intraperitoneal injection of clozapine-N-oxide (CNO) (Fig. 4). The mice with DREAD-Gi expressed in apMPOA-recipient ARC neurons showed lower food intake after CNO injection (1.2 mg/kg) under different ambient temperatures (Fig. 4k). Whereas the chemogenetic inhibition on the transsynaptic PVH neurons induced increased food intake after CNO injection (1.2 mg/kg) (Fig. 4h). No effect of CNO on food intake was observed in control mice with mCherry expressed in the postsynaptic neurons in ARC and PVH (Fig. 4i, l). Consistent with the optogenetic activation and cell ablation, chemogenetic inhibition on the apMPOA→ARC and PVH pathways further identified their regulatory roles on feeding behavior.

It is worth mentioning that within-group comparisons on the food intake of the mice with transsynatic neurons in the ARC and PVH genetically ablated or inhibited among the three ambient temperatures (purple or red bars in Fig. 4c, h), showed different patterns from the controls (e.g., food intake showed the pattern of LT>NT>HT, Fig. 1b and Fig. S1a, gray bars in Fig. 4c, h), suggesting that the ablation or inhibition of the apMPOA→ARC and PVH projections reversely eliminated the temperature-dependence of feeding behavior as observed in the control groups. This finding further proves that apMPOA→ARC and PVH projections play a vital role in the ambient temperature dependence of feeding behavior, whereas cutting off both pathways result in the loss of this property.

5. Thermosensory characteristics of ARC and PVH-projecting neurons in the apMPOA

The manipulations outlined above demonstrate that the apMPOA→ARC/PVH pathways orchestrate feeding behavior. However, it remains unclear whether the apMPOA-innervated circuits regulate feeding behavior by incorporating ambient thermal inputs. Here, we investigated the thermosensory characteristics of ARC/PVH-projecting apMPOA neurons using retrograde tracing and optical photometry. We injected AAVretro-DIO-Flp (mixed with red fluorescent biotinylated dextran amines to indicate the injection range) into the ARC/PVH and Flp-dependent AAV-fDIO-GCaMP6s into the apMPOA of vGluT2-cre mice, and installed an optical fiber above the apMPOA to record calcium responses to two types of stimulations: local stimulation on a thermal plate and ambient exposure in an environmental chamber (Fig. 5a-b). We discovered that the ARC-projecting apMPOA neurons exhibited no calcium responses to local warming (25→40°C) or cooling (25→10°C) on the thermal plate compared with mice subjected to

neutral stimulation (25°C, upper parts in Fig. 5c-f and Fig. S5b-d). The same mice showed obviously elevated calcium activity in a cold chamber (25→10°C), but no responses in a hot chamber (25→35°C, upper parts in Fig. 5h-k and Fig. S5f-h). The PVH-projecting apMPOA neurons showed no calcium response on the hot plate, but relatively reduced one on the cold plate (lower parts of Fig. 5c-e, g and Fig. S5b-d). The same mice showed increased calcium activity in a hot chamber, but reduced one in a cold chamber (lower parts in Fig. 5h-j, l and Fig. S5f-h). These findings suggested that ARC-projecting apMPOA neurons were selectively activated by cooling, and PVH-projecting neurons had bidirectional thermosensory characteristics. Importantly, the PVH and ARC-projecting apMPOA neurons specifically responded to ambient thermal exposure, rather than local thermal stimuli (PVH-projecting neurons showed weak responses to local cooling). These findings were also identified by colocalizations between thermal-induced C-Fos and retrograde traced apMPOA neurons (Fig. S6). The distinct thermosensory characteristics of the two subsets of apMPOA neurons may be the neural basis of ambient temperature dependence of feeding behavior. In sensing external thermal inputs, the apMPOA neurons with distinct thermosensory characteristics orchestrate feeding behavior through fiber projections to anorexigenic or orexigenic neurons that are densely distributed in the PVH and ARC.

6. Anatomical and molecular differentiations of the two populations of apMPOA neurons using projection-specific RNA sequencing

We next sought to explore the evidence for the heterogeneity of the ARC and PVH-projecting neurons in the apMPOA. We first examined their anatomical colocalizations by injecting CTB-555 and CTB-488 into the PVH and ARC respectively (Fig. 6a). The retrograde-labeled neurons from PVH and ARC were sparsely colocalized with each other (approximately 9% of CTB-488+ neurons expressed CTB-555, whereas 14% of CTB-555+ neurons expressed CTB-488), indicating that the ARC and PVH-projecting neurons in the apMPOA were two neighboring but separate populations (Fig. 6b-c).

Given the distinct characteristics in sensing ambient temperatures (Fig. 5h-j), we next investigated their neurotransmission inputs using retrograde rabies virus (RV). We injected Cre-dependent AAVretro vectors expressing EGFP-TVA and RG into the PVH or ARC (not in the same mouse) of vGluT2-cre mice. After allowing three weeks for expression in the retrograde-labeled neurons in apMPOA, we injected the rabies virus RV-EnvA-ΔG-dsRed into the apMPOA (Fig. 6d). With this viral strategy, the RV could specifically label the anatomical inputs to apMPOA neurons that projecting to PVH and ARC. Both PVH and ARC-projecting apMPOA neurons co-received monosynaptic inputs from multiple upstream regions (Fig. S7). Important, their monosynaptic inputs showed a certain distinction. Specifically, strong RV labeling was observed in the posteromedial part of the BNST (pBNST), dorsal subnuclei of lateral parabrachial nucleus (LPBd), nucleus tractus solitaries (NTS), and BA to the PVH-projecting apMPOA neurons (Fig. 6e-f). In contrast, the ARC-projecting apMPOA neurons received sparse inputs from these regions, but numerous inputs from dense cell bodies in the external subnuclei of LPB (LPBe, Fig. 6e, g). Among these upstream regions, the LPB has been previously identified to transmit cutaneous thermosensory signals of ambient temperature, with the LPBd transmitting warming signals to glutamatergic MPOA neurons, whereas the LPBe transmitting cutaneous cooling input to GABAergic neurons in MnPO, thus facilitating

thermoregulation [40,41]. In addition to the LPB, we also found strong RV labeling in the pBNST, NTS, and BA, which are not considered in the current study because they were not previously reported to be involved in thermosensation or transmission [42,43].

To molecularly discriminate the two subsets of ARC/PVH-projecting apMPOA neurons, we collected them in acute sections with a glass pipette after retrograde labeling and sequenced the RNA using SmartSeq2 protocol (Fig. 7a). We injected a Cre-dependent AAVretro vector expressing EGFP into the PVH or ARC (not in the same mouse) of vGluT2-cre mice (Fig. 7a). After allowing three weeks for the expression of EGFP, we dissected acute brain slices containing apMPOA and collected fluorescently labeled cells in the apMPOA with glass pipettes (Fig. 7a). A total of 5 biological repeats were collected for the PVH and ARC groups, respectively, with 15 cells for one mouse sample. A total of 15,682 and 15,889 transcripts were expressed in PVH and ARC-projecting apMPOA neurons, with 765 and 972 transcripts being uniquely expressed in each group (Fig. 7b). A total of 455 significant differentially expressed genes (DEGs) were found, with 221 DEGs upregulated in PVH-projecting apMPOA neurons and 234 DEGs upregulated in ARC-projecting neurons (Fig. 7b-c). We performed gene annotation analysis via KEGG pathway category and investigated potential candidate genes among the top ten DEGs (Fig. 7d-g). We focused on a set of DEGs depending on their functions in metabolism-related cellular processing and intercellular transmission activity, including the genes *Eno1*, *Aplnr*, *Crhr2*, *Htr1f*, *Drd3*, *Irak4*, and *Itgb5* (Fig. 7d-g). We also analyzed a range of genes related to appetite neuropeptides or receptors which might not fall into the top ten of gene annotation analysis above (Fig. 7h), we found that the genes *Htr1f*, *NPY1r*, *GalR1* and *NPY5r* were group-differed. Collectively, we selected the DEGs *Htr1f*, *Irak4*, *Aplnr*, *Itgb5*, *Eno1*, *Crhr2*, *Drd3*, *GalR1*, *Npy1r* and *Npy5r* as candidate marker genes for further behavioral verification (red # in Fig. 7d-h).

We tested behavioral performances of mice after microinjecting inhibitors or agonists of these candidate genes into apMPOA (Fig. 7i). We found that injection of apelin in the apMPOA suppressed food intake of starved mice under normothermia (Fig. 7j). The inhibiting effect of apelin in the apMPOA was robust in response to ambient temperatures (Fig. 7k). Blocking the apelin receptors in the apMPOA during ambient temperature robustly promoted food intake compared with the results of PBS injection (Fig. 7l). A similar feeding pattern induced by pharmacological apelin application with optogenetic/chemogenetic manipulations on apMPOA→PVH pathway indicated that the *Aplnr* might be a potential marker for the PVH-projecting apMPOA neurons. In contrast to the apelin, microinjection of galanin in the apMPOA also increased food intake during normothermia (Fig. 7j). The promoting effect of galanin in the apMPOA was robust under ambient temperatures (Fig. 7k). Conversely, blocking the galanin receptor 1 in the apMPOA reversed the promoting effects of galanin neurons on food intake in response to ambient temperatures (Fig. 7l), suggesting that the *GalR1* might be a potential marker for the ARC-projecting apMPOA neurons. Additionally, NPY injection showed promoting effect during normothermia (Fig. 7j), but not during high or low ambient temperature (Fig. 7k), and blocking the NPY1 receptors in the apMPOA had no effect on feeding (Fig. 7l).

We further performed immunofluorescence to verify the expressions of *Aplnr* and *GalR1* in PVH and ARC-projecting apMPOA neurons. We injected Cre-dependent AAVretro vectors expressing mCherry into the

PVH or ARC (not in the same mouse) of vGluT2-cre mice, and performed immunofluorescence of anti-apelin receptor and anti-galanin receptor 1 three weeks later. The ARC-projecting neurons in the apMPOA exhibited substantial colocalization with galanin receptor 1. Approximately 60% of ARC-projecting neurons expressed galanin receptor 1, but minor colocalization with apelin receptor (Fig. 7m, 7n, 7q). The PVH-projecting apMPOA neurons were primarily overlapped with apelin receptor, but not galanin receptor (50% PVH-projecting apMPOA neurons expressed apelin receptor) (Fig. 7o, 7p, 7r). These findings indicated that the two subsets of ARC-projecting and PVH-projecting apMPOA neurons were molecularly distinct.

Discussion

Here, we discovered a previously unrecognized neuronal populations and circuits for coordinating feeding behavior in coping with ambient temperature. The regulatory effect is centrally orchestrated by two subsets of glutamatergic neurons in the apMPOA projecting to the ARC and PVH. One subset of apMPOA neurons showed an active response to low ambient temperature, enacting a promoting food intake through terminal fibers projecting to the ARC. Conversely, the other subset of glutamatergic neurons, which project to the PVH, inhibited food intake, showing an active response to high ambient temperature. In coping with anatomically heterogeneous ambient thermal inputs from LPB, the two subsets of apMPOA neurons, which were molecularly distinct in terms of apelin and galanin receptor occurrence, adaptively mediated feeding behavior.

Feeding behavior is modulated by the demand of thermal homeostasis

Feeding is a complex innate behavior that maintains energy homeostasis and is regulated by a variety of hard-wired neural circuits [44]. The survival relevant innate behaviors such as hunger, thirst, pain, fear and anxiety, is hierarchically regulated [45-47]. The most urgent environmental or physiological factors are prioritized when they threaten survival [48]. In the instances of thermal challenges, thermal homeostasis tends to be the highest priority process for ensuring survival by all possible means of regulation, such as BAT thermogenesis, shivering, and vascular contraction and dilation [49], regardless of hunger or satiety. As a key means of behavioral thermoregulation [50], the adaptive feeding behavior would help the body defend against extreme thermal challenges. Promoted feeding would provide a greater energy supply in response to cold environments, conversely, the inhibition of feeding would impede extra heat production in a hot environment. From this perspective, we reason that feeding behavior acts as an indispensable mechanism of thermoregulation under extreme ambient temperatures, in which the body regulates the amount of food intake according to the demand for heat production and dissipation, rather than glucostasis or lipostasis [51,52]. The potential contribution of feeding to thermoregulation is easily overlooked under normothermic conditions. However, it cannot be ignored that the coordinating regulatory effect of ambient temperature on feeding is a common phenomenon in rodents at extreme

temperatures [53]. Likewise, feeding in humans shows a certain dependence on temperature, and climate, especially in the soldiers in extreme environments [10-12].

Neural circuits underlying ambient temperature-regulated feeding behavior

The apMPOA comprises multiple cell populations [54], and innervates downstream targets that mediate complex innate behaviors [30,33], and homeostatic regulatory processes [17,34]. Our study further widened the regulatory role of apMPOA in orchestrating temperature-regulated feeding behavior. Overriding energy demand, feeding behavior acts as a mechanism for thermoregulation likely requiring hard-wired neural circuits that intertwine temperature and food signals.

The unique anatomical downstream and upstream targets of apMPOA facilitate rapid sensing and integrating ambient temperature and energy state, and exert a corresponding regulatory role. Anatomically, the apMPOA is located along the third ventricle and extends dense fibers to nearby circumventricular nuclei involved in energy homeostasis, such as DMH, LH, PVH, ARC [30,31]. Among the downstream targets of apMPOA, the PVH is enriched with anorexigenic melanocortin receptors, which induce proopiomelanocortin (POMC) neurons to release anorexigenic α-melanocyte-stimulating hormone (α-MSH) [44,55]; and the ARC, as a key satiety center, is enriched in anorexigenic POMC neurons and feed-promoting NPY/AgRP neurons [37,56,57]. The apMPOA has denser fiber projections to the downstream PVH and ARC, suggesting an anatomical arrangement for temperature-dependent feeding behavior.

We revealed that the neighboring but separate apMPOA neurons received specific upstream inputs from LPB. The PVH-projecting apMPOA neurons receive transsynaptic inputs from LPBd, in contrast, ARC-projecting apMPOA neurons receive anatomical inputs from the LPBe. The LPB-MPOA pathway plays a critical role in transmitting external thermal signals for autonomic thermoregulation [40,41,58-60]. Glutamatergic LPBd neurons transmit warm signals to activate GABAergic MPOA neurons which further suppress thermogenic nuclei. Whereas, cooling signals are transmitted from LPBe neurons to GABAergic MnPO neurons which further inhibit GABAergic MPOA neurons. In addition to GABAergic neurons, glutamatergic neurons in the MPOA also participate in warmth sensation and regulation [8,49]. The activation of glutamatergic neurons in the VMPO that are innervated by glutamatergic terminals from LPB, induces body hypothermia [49]. These pioneering findings delineate that feeding behavior, as a means of behavioral thermoregulation [50], shares the same thermal transmission pathway LPB-MPOA with the canonical autonomic thermoregulation. The MPOA contains diverse cell types and intricate neural circuits that innervate a series of downstream homeostatic-related targets [8,17,34,61]. Supporting this, activation on MPOA neurons induced both temperature and feeding behavior alterations (Fig. 2). We infer that the essential effectors of feeding behavior and autonomic thermoregulation co-orchestrated by apMPOA lie in the distinct downstream regions. Noticeably, the ablations of postsynaptic neurons in DMH led to autonomic thermoregulation deficiency, whereas ablations in PVH and ARC led to alterations of food

intake (Fig. 4 and Fig. S3). These findings revealed an unrecognized neural circuits of temperature-regulated feeding behavior orchestrated by LPB→apMPOA→PVH/ARC pathways.

Molecular mechanisms underlying ambient temperature-regulated feeding behavior

Genetic evidence obtained from projection-specific RNA sequencing showed that the galanin receptor and apelin receptor could be used to molecularly discriminate the two subsets of apMPOA neurons. Galanin receptor neurons are located in multiple hypothalamic nuclei that mediate feeding behavior, including the LH [62], ARC [63], NTS [64], PVH [65], VMH [66], as well as in MPOA [67,68]. Consistent with our findings of hunger-evoked C-Fos expression, galanin receptor neurons in the MPOA were previously reported to be activated by food deprivation [67]. The dense synaptic links between galanin neurons and both NPY and POMC neurons in the ARC [69], and orexin and melanin-concentrating hormone (MCH) neurons in the LH [70,71], supports the regulatory function of galanin on feeding behavior. Here, our findings uncover the functional significance of galanin in the apMPOA in mediating feeding behavior. Galanin receptor neurons were substantially overlapped with apMPOA neurons that specifically project to orexigenic ARC, but not PVH (Fig. 7m-n). Our result suggests that galanin receptor apMPOA neurons→ARC pathway reflects a neural strategy for replenishing energy in response to a cold environment.

Apelin is abundant in hypothalamic nuclei that regulate feeding behavior, including the MPOA, PVH, DMH, ARC, and VMH [72]. The intracerebroventricular injection of apelin inhibits feeding behavior [73-75]. The inhibitory effect of apelin on food intake remains a matter of debate. The hypothalamic corticotropin releasing factor (CRF) system might participate in the apelinergic system, as CRF receptor antagonist could reverse the inhibitory effect of apelin on food intake [73]. Apelin receptor neurons in the hypothalamus are largely colocalized with CRF secreting neurons [76,77]. In another study, apelin receptor neurons were shown to be strongly colocalized with POMC, and to regulate feeding behavior through α-MSH release [72]. Apelin is also expressed in the MPOA [78], however, the specific neuronal function remains unclear. According to our findings, the apelin receptor neurons were largely overlapped with apMPOA neurons that specifically project to anorexigenic neurons in the PVH, but not overlapped with ARC-projecting apMPOA neurons (Fig. 7o-p). This finding suggests that apelin receptor apMPOA neurons→PVH pathway reflects another neural strategy for suppressing energy intake in response to a hot environment.

Ambient peripheral thermal input regulates feeding behavior

In this study, we found that apMPOA neurons showed obvious responses to ambient exposure but not (or weak) to local exposure (Fig. 5d-e, i-j). The way by which central hypothalamus responds to peripheral local or environmental thermal inputs has yet to be fully elucidated. Diverse central responses induced by local body parts and ambient whole body exposure might be attributed to variations in the density,

thresholds, cell types and afferent pathways of cutaneous thermoreceptors [79,80]. Thermosensation and regulation works independently through various scattered thermal effectors related to diverse thermoregulation variables, but not be completed by a central integrator [79,81]. In terms of the central system, multiple neural circuits exist in the brain, where each thermoregulatory effector system is driven by its own peripheral thermal sensors. For example, local warming or cooling on hands induces local thermal intensity sensation and vascular activity, rather than BAT thermogenesis, or shivering [82,83]. Particularly, local warming or cooling on face or head differs from other sites (hand, leg, etc.), producing changes in higher cognitive or emotional aspects [84,85]. Whereas, ambient thermal exposure results in diverse thermoregulation variables, such as vasodilation, locomotion, energy expenditure, BAT thermogenesis, shivering [49,61,86,87]. In current study, the coordinating feeding behavior innervated by apMPOA acts as a means of behavioral thermoregulation to maintain energy homeostasis [50], only in coping with ambient challenges that probably disrupt the homeostasis, but not in response to the local thermal sensory or pain that usually would not affect energy homeostasis. This property of apMPOA-innervated pathways suggests an evolutionarily conserved regulatory role of temperature on feeding behavior only in the case of ambient challenges.

Conclusions

In summary, we identified the apMPOA as a previously unknown structure that intertwines ambient temperature and food. In receiving distinct synaptic inputs from the LPB, the PVH and ARC-projecting apMPOA neurons that express apelin and galanin receptors orchestrate feeding behavior in coping with ambient thermal challenges. By developing a physiological understanding of the ambient temperature-regulated feeding behavior, this study provides a probable entry point for studying neural mechanisms of feeding disturbance of patients with pathological POA lesions, as well as fever-induced anorexia.

Methods

Animals

Mice were group housed under a 12-hour light-dark cycle with ad libitum access to food and water unless otherwise noted. Adult male and female (aged 2-3 months) C57BL/6J, Ai9 (Cre-dependent tdTomato reporter) mice, (Jackson Laboratories, Stock No. 007909), vGluT2-IRES-Cre mice (Jackson Laboratories, Stock No. 016963), and GAD2-IRES-cre mice (Jackson Laboratories, Stock No. 010802) were used in this study. All experimental procedures were approved by the Animal Care and Use Committee of Army Medical University.

Stereotactic virus injection and optical fiber implantation

The present study used mice at approximately 2 months of age, with balanced numbers of males and females. After anesthesia with a mixture of ketamine (55 mg/kg) and xylazine (6.4 mg/kg), the hairs on the scalp of mice were shaved off. Erythromycin ointment was rubbed on the eyes of the mice. Then, the mice were fixed on a stereotaxic device. For the study of retrograde calcium signaling in the apMPOA→ARC pathway in response to a thermal stimulus (Fig. 5), adeno-associated virus AAVretro-Flp (AAV2/retro-DIO-Flp, 5.79×10^{12} vg/mL), which expresses recombinant enzymes retrogradely, was injected 60-65 nL unilaterally at a rate of 25 nL/min at the site of the ARC, with the injection coordinates: AP=-1.7 mm, ML=0.25 mm, DV=5.65-5.7 mm, with the glass electrode left in place for about 10 minutes and then withdrawn. Then the glass electrode was replaced and filled with mineral oil. The Cre-dependent GCaMP6s virus (AAV2/8-EF1a-fDIO-GCaMP6s, 5.14×10^{12} vg/mL, 100-120 nL), was aspirated and injected unilaterally in the apMPOA at a rate of 25 nL/min, with the injection coordinates: AP=+0.45 mm, ML=0.25 mm, DV=4.9-5.0 mm. In the experiment of calcium signaling of apMPOA to altered dietary states (Fig. 1k), the Cre-dependent GCaMP6s virus (AAV2/8-EF1a-DIO-GCaMP6s, 5.94×10^{12} vg/mL) was injected into the apMPOA of vGluT2-ires-cre mice. After virus injection, an optical fiber was placed 200-300 μm over the apMPOA at AP= +0.45mm, ML=0.25 mm, DV=4.5 mm. After the placement of optical fiber, two skull screws were fixed firmly in the skull surface. Then the fiber and screws were completely covered with dental cement. The gripper holding the fiber was removed after the cement had set. The mice were returned to their home cages and housed for 2-3 weeks before testing. For the optogenetic experiment (Fig. 2a and Fig. 3a), the Cre-dependent hChR2 virus (AAV2/8-EF1a-DIO-hChR2-EYFP, 1.33×10^{13} vg/mL) was injected into the bilateral apMPOA of vGluT2-cre mice. Allowing 4 weeks for virus expression, two optical fibers were placed above the apMPOA or its target areas. The detailed coordinates for fiber placements were as follows: apMPOA: AP=+0.45 mm, ML=±2.0 mm, angle of deflection=22°, DV=4.65 mm; PVH: AP=-0.7 mm, ML=±1.5 mm, angle of deflection=16°, DV=4.3 mm; PVT: AP=-1.22 mm, ML=±1.0 mm, angle of deflection=19°, DV=2.7 mm; ARC: AP= -1.7 mm, ML=±2.3 mm, angle of deflection=21°, DV=5.5 mm; LH: AP= -1.3 mm, ML=±2.0 mm, angle of deflection=10.5°, DV=4.5 mm; TN: AP= -1.58 mm, ML=±1.5 mm, angle of deflection=5.5°, DV=5.15 mm; VTA: AP= -3.28 mm, ML=±1.5 mm, angle of deflection=14°, DV=4.0 mm; PAG: AP=-2.7 mm, ML=0.25 mm, DV=2.5 mm; DMH: AP=-1.8 mm, ML=±1.5 mm, angle of deflection=12°, DV=4.8 mm; BNST: AP= +0.5 mm, ML=±2.0 mm, angle of deflection=21°, DV=3.1 mm; BA: AP=-2.54 mm, ML=±2.75 mm, DV=3.8 mm. In the experiment of genetic ablating postsynaptic neurons of apMPOA (Fig. 4a), a high titer of AAV1-cre-GFP was injected into the bilateral apMPOA with 200 nL in total (1.12×10^{13} vg/mL). The Cre-dependent vector AAV-flex-taCasp3-TEVp was respectively injected into bilateral ARC (at the above injection coordinates, 6.73×10^{12} vg/mL, 65nL), PVH (at the above injection coordinates, 65nL/unilateral), and DMH (AP=-1.8 mm, ML=±0.32 mm, DV=5.5 mm, 80 nL/unilateral). In the experiment of chemogenetic inhibition of PVH and ARC neurons, the Cre-dependent vector AAV2/9-DIO-hM4Di-mCherry encoding inhibitory Designer Receptors Exclusively Activated by Designer Drugs (DREADDs, hM4Di) was respectively injected into the bilateral ARC (at the above injection coordinates, 3.6×10^{12} vg/mL, 65nL), PVH (at the above injection coordinates, 65nL/unilateral).

Temperature exposure test

To assess the calcium activity of the apMPOA induced by thermal stimulation, two thermal stimulation approaches were designed. One involved the application of a localized temperature stimulus on an aluminum plate via semiconductor cooling/heating. The mice could move around on the aluminum plate, and local temperature stimulation was applied on their feet when the temperature changed. The temperature of hot plate and cold plate were designed as 40°C and 10°C according to previous studies [17,32]. In the other method, mice were subjected to whole-body temperature exposure in thermostatically controlled chambers. In contrast to the thermal plate temperatures, the temperatures of the two chambers were set at 35°C and 10°C to avoid overheating-induced mania or death. The preset temperatures of the thermal plates and chambers could be quickly reached from room temperature 25°C in about 3 minutes via semiconductor temperature control module.

Temperature recording

Rectal temperature was measured by using a high-sensitivity digital thermometer (GM1365) with a precision of 0.1°C. We inserted the tip of the thermometer into the mouse anus and recorded the temperature reading while it remained steady. The BAT temperature was dynamically monitored with an infrared imager (FLIR ONE). The infrared imager was turned on for dynamic video recording when the mice were optogenetically stimulated. After the experiment, infrared images at the specified time points were captured.

Fiber photometry

In the present study, the calcium activity in the apMPOA induced by fasting and ambient temperature exposure was recorded using a fiber photometry system (C1410488, Inper, Hangzhou). The ceramic ferrules placed into the mouse brain were connected to 410 nm and 488nm laser. The activity-dependent GCaMP6s fluorescence signal (488 nm) and activity-independent fluorescence (410 nm) were all captured by a CMOS camera, providing internal control for movement and bleaching artifacts. For $\Delta F/F$ calculation, baseline F_0 was defined as the average F during 4 minutes before feeding behavior was initiated in the fasting-induced calcium activity recording experiment, and F_0 was defined as the average F during 5 minutes before the ambient temperature was changed in the temperature-induced calcium activity recording experiment.

Feeding behavior test

Wild type mice were deprived of food, but not water, overnight (8:00 pm-8:00 am +1). In the fasting-induced C-Fos experiment, the re-feeding group was presented with standard chow for 2 hours after overnight fasting, while the fasting group was not presented with chow. The no-fasted group was not deprived of food. Two hours later, the three groups were all sacrificed and perfused. In the optogenetic, chemogenetic and ablation experiments, the mice were deprived of food, but not water, for 12 hours (8:00 am -8:00 pm). Then they were presented with the standard mouse chow in the feeders. Two-hour food intake was recorded. Regarding food intake during ambient temperature exposure, both two-hour and twelve-hour food intake were all recorded after fasting from 8:00 am to 8:00 pm. In the fiber photometry experiment of calcium signals in response to dietary state, the mice were fasted for 24 hours in order to ensure that they would eat during the recording process.

To avoid leaving behind chow crumbs and mixing with mouse droppings and urine, a mouse feeder was designed. We drilled four semicircular holes in two rectangular copper blocks (designed according to the feed diameter, 9 mm). The size of the copper block was 8 cm×1 cm×2.5 cm. The chow was placed into the semicircular holes, and the two copper blocks are then tightened with bolts. The length of chow protruding from the copper did not exceed 6 mm. In order to collect chow crumbs, a narrow metal trough under the copper block was designed. The size of the metal trough was 8 cm×1.5 cm×0.5 cm. After feeding behavior test, the remaining intact chow and crumbs are weighed together and the difference in weight from the pre-feeding weight was calculated as the food intake.

Immunohistochemistry

The mice were anesthetized by the intraperitoneal injection of 25% urethane (1.5 mg/kg). Then, they were perfused with 0.1 M PBS, followed by 4% paraformaldehyde (PFA). After the mouse was well fixed, the mouse brain tissue was removed and placed in 4% PFA overnight for further fixation. The brain tissue was immersed in 10% sucrose solution (4% PFA) on the following day and dehydrated for 2 days. For complete dehydration we immersed the tissue in 20% and 30% sucrose solution for gradient dehydration. The brains were frozen and sectioned into 30 μm slices. In the C-Fos staining experiment, after washing in 0.1 M PBS with 0.3% Triton-X 100 for 30 minutes and blocking with 10% goat serum for 1 hour at 37°C, the sections were incubated with the primary antibody, anti-cFos (1:1000, rabbit, ab190289, Abcam), at 37°C for 30 min and then at 4°C overnight. After washing in 0.1 M PBS for 30 minutes, the sections were incubated with a fluorescent secondary antibody (goat anti-rabbit 488, 1:500, ab150077, Abcam) at 37°C for 1 hour. In the galanin receptor 1 staining in apMPOA, the sections were blocked with 10% horse serum for 1 hour at 37°C, and then incubated with the primary antibody, anti-galanin receptor 1 (GalR1, 1:50, rabbit, LSBio, LS-C120666) at 37°C for 30 min and then at 4°C overnight. After washing in 0.1 M PBS for 30 minutes, the sections were incubated with a fluorescent secondary antibody (donkey anti-rabbit 488, 1:2000, ab150073, Abcam) at 37°C for 1 hour. In the apelin receptor staining in apMPOA, the sections were blocked with 10% goat serum for 1 hour at 37°C, and then incubated with the primary antibody, anti-apelin receptor (1:200, rabbit, Invitrogen, PA5-114830) at 37°C for 30 min and then at

4°C overnight. After washing in 0.1 M PBS for 30 minutes, the sections were incubated with a fluorescent secondary antibody (goat anti-rabbit 488, 1:2000, ab150077, Abcam) at 37°C for 1 hour. Finally, all the sections were stained with DAPI at room temperature for 10 minutes and washed in 0.1 M PBS for 30 minutes.

Anterograde-Tracing

A Cre-dependent rAAV expressing the hChR2-eYFP protein (AAV8-EF1α-DIO-hChR2-eYFP) was bilaterally injected into the apMPOA (120 nL per side). After injection, the mice were returned to their home cages and kept for 4 weeks. The animals were sacrificed after night fasting (8:00 pm-8:00 am+1) and processed for C-Fos immunohistochemical staining.

Retrograde labeling

To retrogradely label the neurons in the apMPOA from the PVH and ARC, we injected the AAVretro-cre virus into the PVH and ARC of Ai9 respectively (5.24×10^{12} vg/mL, 65 nL). The Cre recombinase was expressed retrogradely from the fiber terminals to the cell bodies in the apMPOA and combined with the fluorescent protein tdTomato. The labeled cell bodies were further quantified for the colocolizations with the C-Fos induced by thermal stimulations.

To differentiate the neurons in the apMPOA that project to the PVH and ARC, we likewise injected 65 nL of CTB-555 and CTB-488 into the PVH and ARC respectively in wild-type mice. The two CTBs were retrogradely expressed from the terminals to cell bodies in the apMPOA. The colocalization of neurons projecting to the PVH and ARC was quantified.

To explore the upstream inputs of PVH and ARC-projecting apMPOA neurons, we performed monosynaptic retrograde labeling using modified rabies virus. The helper viruses AAVretro-DIO-TVA-EGFP and AAVretro-DIO-oRVG were mixed in equal volumes and 70 nL of the mixture was then unilaterally injected into the ARC and PVH of vGluT2-cre mice respectively (5.24×10^{12} vg/mL). After expression for three weeks, the rabies virus RV-ENVA-ΔG-dsRed (2.5×10^{8} IFU/mL, 100 nL) was injected into the apMPOA. Then, the mice were returned to their home cages. After one week of viral replication, the mice were sacrificed and their brains were prepared for further imaging.

Projection-specific RNA sequencing

To molecularly differentiate the neurons in the apMPOA projecting to the ARC and PVH respectively, we performed transcriptome sequencing using the SmartSeq2 protocol [88]. The neurons in the apMPOA were

specifically labeled by the injection of Cre-dependent AAVretro-DIO-EGFP into the ARC and PVH of vGluT2-cre mice (3.8×10^{12} vg/mL). After allowing three weeks for the expression of EGFP, the mice were sacrificed and their brains were quickly removed and submerged into ice-cold ACSF. Then the brains were cut into 300 μm-thick coronal slices containing the apMPOA, PVH or ARC. The slices containing apMPOA were incubated in N-methyl-D-glucamine (NMDG)-incubation fluid (110 NMDG, 110HCl, 2.5 KCl, 1.2 NaH_2PO_4, 25 Glucose, 10 $MgSO_4$, 0.5 CaCl2 and 25 $NaHCO_3$ in mM) for 15 minutes at 32°C. Then the slices were transferred to oxygen-saturated ACSF and incubated for 1 hour at room temperature. After incubation, the slices were transferred to the recording chamber of an electrophysiological recording platform. Oxygen-saturated ACSF was continuously perfused.

To collect fluorescently labeled neurons, glass pipettes of 2-4 MΩ were used to suck the neurons under a microscope. The pipettes were filled with sterile PBS and a slight positive pressure was given before attaching the cell. The pipette tip approached the cell from the side of the cell, rather than from the top. Once the tip touched the cell, we quickly removed the positive pressure and gave a light negative pressure until the cell had been visibly sucked into the tip. Then, we locked in the negative pressure and raised the pipette away from the brain slice. We broke the tip of the pipette into a PCR tube containing 4 μl RNase inhibitor in lysis buffer. The PCR tube was store on ice until 15 cells were collected for one mouse sample. Then the tube was transferred to -80℃ ultra-low refrigerator. A total of five biological repeats were collected for the PVH and ARC groups respectively.

The SmartSeq2 protocol was used to perform RNA sequencing. The samples were incubated at 72°C, and immediately returned to the ice. Then the samples were reversely transcribed to cDNA based on the polyA tail and amplified the full-length cDNA by PCR. RNA degradation and contamination were monitored by 1% agarose electrophoresis. The library construction was prepared according to the Tagmentation-based library protocol. The PCR products were purified and selected with the Agencourt AMPure XP-Medium kit. DNA was quantified with an Agilent Technologies 2100 bioanalyzer. Then the library was amplified to generate DNA nanoball (DNB), containing more than 300 copies of a single molecule. The DNBs were loaded into the patterned nanoarray and single end 50 bases reads were generated in the way of sequenced by combinatorial Probe-Anchor Synthesis (cPAS).

HISAT2 (v2.0.4) was used to map the reads to the mouse genome for transcript abundance quantification. Transcripts per kilobase of exon model per million mapped reads (TPM) or fragments/kbp of transcript/million mapped reads (FPKM) values of each gene were calculated based on the length of the gene and the number of reads mapped to the gene. The correlational analysis, enrichment analysis and clustering analysis of DEGs were carried out on the Dr. Tom system. DESeq2 was conducted to identify DEGs between the ARC and PVH groups, and significant DEGs were selected as fold change≥2 and q≤0.05. The resulted DEGs were annotated using the databases such as the NCBI, Gene Ontology (GO), and Kyoto Encyclopedia of Genes and Genomes (KEGG) to obtain further information.

Pharmacological experiments

In pharmacological experiments of injecting agonists and antagonists of candidate genes, wild-type mice were implanted with cannulas above the bilateral apMPOA (AP= +0.45 mm, ML=±2.0 mm, angle of deflection=22°, DV=4.7 mm) which were secured to the skull with screws and dental cement. Then the mice were returned to home cages and housed for 1 week for recovery. Before behavioral testing, the mice were habituated to handling, injection and food feeder for 2 hours every day. Drugs were diluted from frozen aliquots before each experiment and were then microinjected (150 nL/unilateral) into the apMPOA with an internal cannula connected to a microliter syringe pump. Fifteen minutes after bilateral injections, the mice were returned to their home cages and feeding behavior tests were performed for 2 hours. The drugs were prepared fresh on the day of the experiment by dilution in vehicle solution (PBS supplemented with 0.1% DMSO, 5% PEG400 and 5% Tween-80), including the integrin inhibitor SB273005 (Selleck, 150 nL/unilateral, 1 μM), the enolase inhibitor AP-III-a4 (ENOblock, Selleck, 150 nL/unilateral, 1 μM), the IRAK4 inhibitor PF-06650833 (Selleck, 150 nL/unilateral, 1 μM), the antagonist of apelin receptor ML221 (Selleck, 150 nL/unilateral, 1 μM), the serotonin reuptake inhibitor Fluvoxamine maleate (MK-264, Selleck, 150 nL/unilateral, 1 μM), the antagonist of dopamine D3 receptor BP897 (Adooq Bioscience, 150 nL/unilateral, 1 μM), the antagonist of NPY Y1 receptor BIBO 3304 trifluoroacetate (Tocris, 150 nL/unilateral, 1 μM) and antagonist of galanin receptor M40 (Tocris, 150nL/unilateral, 1 μM). Bioactive neuropeptides were prepared fresh by dilution in sterile PBS, including apelin receptor agonist apelin-13 (Tocris, 150 nL/unilateral, 1 μM), neuropeptide Y (Tocris, 150 nL/unilateral, 1 μM) and galanin receptor agonist galanin(1-29) (Tocris, 150 nL/unilateral, 1 μM).

Statistics

Animals were randomly assigned to control and treatment groups. For animals with multiple treatments, the sequence of treatments was randomized. Data are represented as mean ± standard error of the mean (SEM). SPSS 18.0 and Prism 8 software (GraphPad) were used for statistical analysis and graphing. T test, paired t test, one-way ANOVA and two-way repeated-measure ANOVA and post hoc least significant difference (LSD) multiple comparisons were used to test significance between samples. Significance was defined at a level of $P < 0.05$.

Declarations

Acknowledgements

This work was supported by grant to Yi Zhou by the National Natural Science Foundation of China (Grant No. 31771152). Dr. Zhen Zhao and Xinying Guo at University of Southern California for generous help with RNA sequencing experiments. Dr. Min Xu at Institute of Neuroscience, Chinese Academy of Sciences and Dr. Xiaowei Chen at Army Medical University for help with the manuscript writing.

Author contributions

Y.Z., Y.X. and S.Q. conceived the study. S.Q., S.Y. and R.P. performed most behavioral experiments. J.Z. and K.L. designed the thermal plate and chamber. S.Q., Z.S., Z.W. and T.L. contributed to recording experiments. Y.J.Z. and S.Q. contributed to data analysis. P.C. and S.Q. contributed to anatomical experiments. Y.Z. and Y.X. supervised the project. Y.Z., Y.X. and S.Q. wrote the manuscript.

Declaration of Interests

The authors declare no competing interests

References

1 Betley, J. N., Cao, Z. F., Ritola, K. D. & Sternson, S. M. Parallel, redundant circuit organization for homeostatic control of feeding behavior. *Cell* **155**, 1337-1350, doi:10.1016/j.cell.2013.11.002 (2013).

2 Zhu, C. *et al.* Somatostatin Neurons in the Basal Forebrain Promote High-Calorie Food Intake. *Cell reports* **20**, 112-123, doi:10.1016/j.celrep.2017.06.007 (2017).

3 Land, B. B. *et al.* Medial prefrontal D1 dopamine neurons control food intake. *Nature neuroscience* **17**, 248-253, doi:10.1038/nn.3625 (2014).

4 Sweeney, P., Li, C. & Yang, Y. Appetite suppressive role of medial septal glutamatergic neurons. *Proceedings of the National Academy of Sciences of the United States of America* **114**, 13816-13821, doi:10.1073/pnas.1707228114 (2017).

5 Deem, J. D. *et al.* Cold-induced hyperphagia requires AgRP neuron activation in mice. *eLife* **9**, doi:10.7554/eLife.58764 (2020).

6 Nakamura, Y. & Nakamura, K. Central regulation of brown adipose tissue thermogenesis and energy homeostasis dependent on food availability. *Pflugers Archiv : European journal of physiology* **470**, 823-837, doi:10.1007/s00424-017-2090-z (2018).

7 Tansey, E. A. & Johnson, C. D. Recent advances in thermoregulation. *Advances in physiology education* **39**, 139-148, doi:10.1152/advan.00126.2014 (2015).

8 Yu, S. *et al.* Glutamatergic Preoptic Area Neurons That Express Leptin Receptors Drive Temperature-Dependent Body Weight Homeostasis. *The Journal of neuroscience : the official journal of the Society for Neuroscience* **36**, 5034-5046, doi:10.1523/JNEUROSCI.0213-16.2016 (2016).

9 Brobeck, J. R. Food Intake as a Mechanism of Temperature Regulation. *Yale Journal ofBiology and Medicine* **20**, 545-552 (1948).

10 Johnson, R. E. & Kark, R. M. Environment and Food Intake in Man. *Science* **105**, 378-379, doi:10.1126/science.105.2728.378 (1947).

11 Mandic, I. *et al.* The effects of exercise and ambient temperature on dietary intake, appetite sensation, and appetite regulating hormone concentrations. *Nutrition & metabolism* **16**, 29, doi:10.1186/s12986-019-0348-5 (2019).

12 Johnson, C. D. *et al.* Energy expenditure and intake during Special Operations Forces field training in a jungle and glacial environment. *Applied physiology, nutrition, and metabolism = Physiologie appliquee, nutrition et metabolisme* **43**, 381-386, doi:10.1139/apnm-2017-0622 (2018).

13 Suwanapaporn, P., Chaiyabutr, N. & Thammacharoen, S. A low degree of high ambient temperature decreased food intake and activated median preoptic and arcuate nuclei. *Physiology & behavior* **181**, 16-22, doi:10.1016/j.physbeh.2017.08.027 (2017).

14 Spector, N. H., Brobeck, J. R. & Hamilton, C. L. Feeding and core temperature in albino rats: changes induced by preoptic heating and cooling. *Science* **161**, 286-288 (1968).

15 Hamilton, C. L. & Brobeck, J. R. Food Intake and Temperature Regulation in Rats with Rostral Hypothalamic Lesions. *The American journal of physiology* **207**, 291-297, doi:10.1152/ajplegacy.1964.207.2.291 (1964).

16 Yu, S. *et al.* Preoptic leptin signaling modulates energy balance independent of body temperature regulation. *eLife* **7**, doi:10.7554/eLife.33505 (2018).

17 Tan, C. L. *et al.* Warm-Sensitive Neurons that Control Body Temperature. *Cell* **167**, 47-59 e15, doi:10.1016/j.cell.2016.08.028 (2016).

18 Hrvatin, S. *et al.* Neurons that regulate mouse torpor. *Nature* **583**, 115-121, doi:10.1038/s41586-020-2387-5 (2020).

19 Takahashi, T. M. *et al.* A discrete neuronal circuit induces a hibernation-like state in rodents. *Nature* **583**, 109-114, doi:10.1038/s41586-020-2163-6 (2020).

20 Andersson, B. & Larsson, B. Influence of local temperature changes in the preoptic area and rostral hypothalamus on the regulation of food and water intake. *Acta physiologica Scandinavica* **52**, 75-89, doi:10.1111/j.1748-1716.1961.tb02203.x (1961).

21 Hamilton, C. L. & Brobeck, J. R. Food intake and activity of rats with rostral hypothalamic lesions. *Proc Soc Exp Biol Med* **122**, 270-272, doi:10.3181/00379727-122-31108 (1966).

22 Mascarenhas, J. F. Role of medial preoptic area (MPOA) in the reproductive function and feeding behavior in rats. *Indian journal of physiology and pharmacology* **30**, 232-240 (1986).

23 Banet, M. F. & Seguin, J. J. Effects of preoptic cooling in rats acclimated to 21 and 4 degree C. *J Appl Physiol* **29**, 385-388, doi:0.1152/jappl.1970.29.3.385 (1970).

24 Ingram, D. L. Effects of heating and cooling the hypothalamus on food intake in the pig. *Brain research* **11**, 714-716, doi:10.1016/0006-8993(68)90165-0 (1968).

25 Zhang, Z. *et al.* Estrogen-sensitive medial preoptic area neurons coordinate torpor in mice. *Nature communications* **11**, 6378, doi:10.1038/s41467-020-20050-1 (2020).

26 Kaltsas, G. A. *et al.* Hypothalamo-pituitary abnormalities in adult patients with langerhans cell histiocytosis: clinical, endocrinological, and radiological features and response to treatment. *The Journal of clinical endocrinology and metabolism* **85**, 1370-1376, doi:10.1210/jcem.85.4.6501 (2000).

27 Roemmler-Zehrer, J. *et al.* Food intake regulating hormones in adult craniopharyngioma patients. *European journal of endocrinology* **170**, 627-635, doi:10.1530/EJE-13-0832 (2014).

28 Roth, C. L., Gebhardt, U. & Muller, H. L. Appetite-regulating hormone changes in patients with craniopharyngioma. *Obesity (Silver Spring)* **19**, 36-42, doi:10.1038/oby.2010.80 (2011).

29 Slawski, B. A. & Buntin, J. D. Preoptic area lesions disrupt prolactin-induced parental feeding behavior in ring doves. *Hormones and behavior* **29**, 248-266, doi:10.1006/hbeh.1995.1018 (1995).

30 Zhang, G. W. *et al.* Medial preoptic area antagonistically mediates stress-induced anxiety and parental behavior. *Nature neuroscience* **24**, 516-528, doi:10.1038/s41593-020-00784-3 (2021).

31 Simerly, R. B. & Swanson, L. W. Projections of the medial preoptic nucleus: a Phaseolus vulgaris leucoagglutinin anterograde tract-tracing study in the rat. *The Journal of comparative neurology* **270**, 209-242, doi:10.1002/cne.902700205 (1988).

32 Zheng-Dong Zhao, W. Z. Y., Cuicui Gao, Xin Fu, Wen Zhang,Qian Zhou, Wanpeng Chen, Xinyan Ni, Jun-Kai Lin, Juan Yang, Xiao-Hong Xu, Wei L. Shen. A hypothalamic circuit that controls body temperature. *Proceedings of the National Academy of Sciences of the United States of America* **114**, E1755, doi:10.1073/pnas.1701881114 (2017).

33 Li, X. Y. *et al.* AGRP Neurons Project to the Medial Preoptic Area and Modulate Maternal Nest-Building. *The Journal of neuroscience : the official journal of the Society for Neuroscience* **39**, 456-471, doi:10.1523/JNEUROSCI.0958-18.2018 (2019).

34 Morrison, S. F., Madden, C. J. & Tupone, D. Central neural regulation of brown adipose tissue thermogenesis and energy expenditure. *Cell metabolism* **19**, 741-756, doi:10.1016/j.cmet.2014.02.007 (2014).

35 Sutton, A. K. *et al.* Control of food intake and energy expenditure by Nos1 neurons of the paraventricular hypothalamus. *The Journal of neuroscience : the official journal of the Society for Neuroscience* **34**, 15306-15318, doi:10.1523/JNEUROSCI.0226-14.2014 (2014).

36 Pei, H., Sutton, A. K., Burnett, K. H., Fuller, P. M. & Olson, D. P. AVP neurons in the paraventricular nucleus of the hypothalamus regulate feeding. *Molecular metabolism* **3**, 209-215, doi:10.1016/j.molmet.2013.12.006 (2014).

37 Aponte, Y., Atasoy, D. & Sternson, S. M. AGRP neurons are sufficient to orchestrate feeding behavior rapidly and without training. *Nature neuroscience* **14**, 351-355, doi:10.1038/nn.2739 (2011).

38 Jennings, J. H. *et al.* Visualizing hypothalamic network dynamics for appetitive and consummatory behaviors. *Cell* **160**, 516-527, doi:10.1016/j.cell.2014.12.026 (2015).

39 Dimicco, J. A. & Zaretsky, D. V. The dorsomedial hypothalamus: a new player in thermoregulation. *American journal of physiology. Regulatory, integrative and comparative physiology* **292**, R47-63, doi:10.1152/ajpregu.00498.2006 (2007).

40 Nakamura, K. & Morrison, S. F. Central efferent pathways for cold-defensive and febrile shivering. *The Journal of physiology* **589**, 3641-3658, doi:10.1113/jphysiol.2011.210047 (2011).

41 Nakamura, K. & Morrison, S. F. A thermosensory pathway that controls body temperature. *Nature neuroscience* **11**, 62-71, doi:10.1038/nn2027 (2008).

42 Stefanos, S., Giada, S., Grace, L. & David, J. A. Experience-dependent plasticity in an innate social behavior is mediated by hypothalamic LTP. *Proceedings of the National Academy of Sciences of the United States of America* **117**, 25789-25799, doi:10.1073/pnas.2011782117/-/DCSupplemental (2020).

43 Sato, K. *et al.* Amygdalohippocampal Area Neurons That Project to the Preoptic Area Mediate Infant-Directed Attack in Male Mice. *The Journal of neuroscience : the official journal of the Society for Neuroscience* **40**, 3981-3994, doi:10.1523/JNEUROSCI.0438-19.2020 (2020).

44 Sohn, J. W., Elmquist, J. K. & Williams, K. W. Neuronal circuits that regulate feeding behavior and metabolism. *Trends in neurosciences* **36**, 504-512, doi:10.1016/j.tins.2013.05.003 (2013).

45 Alhadeff, A. L. *et al.* A Neural Circuit for the Suppression of Pain by a Competing Need State. *Cell* **173**, 140-152 e115, doi:10.1016/j.cell.2018.02.057 (2018).

46 Burnett, C. J. *et al.* Hunger-Driven Motivational State Competition. *Neuron* **92**, 187-201, doi:10.1016/j.neuron.2016.08.032 (2016).

47 Padilla, S. L. *et al.* Agouti-related peptide neural circuits mediate adaptive behaviors in the starved state. *Nature neuroscience* **19**, 734-741, doi:10.1038/nn.4274 (2016).

48 Jikomes, N., Ramesh, R. N., Mandelblat-Cerf, Y. & Andermann, M. L. Preemptive Stimulation of AgRP Neurons in Fed Mice Enables Conditioned Food Seeking under Threat. *Current biology : CB* **26**, 2500-2507, doi:10.1016/j.cub.2016.07.019 (2016).

49 Yang, W. Z. *et al.* Parabrachial neuron types categorically encode thermoregulation variables during heat defense. *Science advances* **6**, doi:10.1126/sciadv.abb9414 (2020).

50 Flouris, A. D. Functional architecture of behavioural thermoregulation. *European journal of applied physiology* **111**, 1-8, doi:10.1007/s00421-010-1602-8 (2011).

51 Mayer, J. The glucostatic theory of regulation of food intake and the problem of obesity. *Bulletin. New England Medical Center* **14**, 43-49 (1952).

52 Kennedy, G. C. The role of depot fat in the hypothalamic control of food intake in the rat. *Proceedings of the Royal Society of London. Series B, Biological sciences* **140**, 578-596, doi:10.1098/rspb.1953.0009 (1953).

53 Brobeck, J. R. Food intake as a mechanism of temperature regulation. *Yale J. Biol. Med* **20**, 545-552 (1948).

54 Moffitt, J. R. *et al.* Molecular, spatial, and functional single-cell profiling of the hypothalamic preoptic region. *Science* **362**, doi:10.1126/science.aau5324 (2018).

55 Xu, Y., Elmquist, J. K. & Fukuda, M. Central nervous control of energy and glucose balance: focus on the central melanocortin system. *Annals of the New York Academy of Sciences* **1243**, 1-14, doi:10.1111/j.1749-6632.2011.06248.x (2011).

56 Garfield, A. S. *et al.* A neural basis for melanocortin-4 receptor-regulated appetite. *Nature neuroscience* **18**, 863-871, doi:10.1038/nn.4011 (2015).

57 Atasoy, D., Betley, J. N., Su, H. H. & Sternson, S. M. Deconstruction of a neural circuit for hunger. *Nature* **488**, 172-177, doi:10.1038/nature11270 (2012).

58 Nakamura, K. & Morrison, S. F. A thermosensory pathway mediating heat-defense responses. *Proceedings of the National Academy of Sciences of the United States of America* **107**, 8848-8853, doi:10.1073/pnas.0913358107 (2010).

59 Kobayashi, A. & Osaka, T. Involvement of the parabrachial nucleus in thermogenesis induced by environmental cooling in the rat. *Pflugers Archiv : European journal of physiology* **446**, 760-765, doi:10.1007/s00424-003-1119-7 (2003).

60 Geerling, J. C. *et al.* Genetic identity of thermosensory relay neurons in the lateral parabrachial nucleus. *Am J Physiol-Reg I* **310**, R41-R54, doi:10.1152/ajpregu.00094.2015 (2016).

61 Wang, T. A. *et al.* Thermoregulation via Temperature-Dependent PGD2 Production in Mouse Preoptic Area. *Neuron* **103**, 309-322 e307, doi:10.1016/j.neuron.2019.04.035 (2019).

62 Qualls-Creekmore, E. *et al.* Galanin-Expressing GABA Neurons in the Lateral Hypothalamus Modulate Food Reward and Noncompulsive Locomotion. *The Journal of neuroscience : the official journal of the Society for Neuroscience* **37**, 6053-6065, doi:10.1523/JNEUROSCI.0155-17.2017 (2017).

63 Hagen, C. J. *et al.* Stimulation of food intake after central galanin is associated with arcuate nucleus activation and does not differ between genetically selected low and high body weight lines of chickens. *Neuropeptides* **47**, 281-285, doi:10.1016/j.npep.2012.11.003 (2013).

64 Sergeant, L., Rodriguez-Dimitrescu, C., Barney, C. C. & Fraley, G. S. Injections of Galanin-Like Peptide directly into the nucleus of the tractus solitarius (NTS) reduces food intake and body weight but increases metabolic rate and plasma leptin. *Neuropeptides* **62**, 37-43, doi:10.1016/j.npep.2016.12.009 (2017).

65 Kyrkouli, S. E., Stanley, B. G. & Leibowitz, S. F. Galanin: stimulation of feeding induced by medial hypothalamic injection of this novel peptide. *European journal of pharmacology* **122**, 159-160, doi:10.1016/0014-2999(86)90175-5 (1986).

66 Schick, R. R. *et al.* Effect of galanin on food intake in rats: involvement of lateral and ventromedial hypothalamic sites. *The American journal of physiology* **264**, R355-361, doi:10.1152/ajpregu.1993.264.2.R355 (1993).

67 Knight, Z. A. *et al.* Molecular profiling of activated neurons by phosphorylated ribosome capture. *Cell* **151**, 1126-1137, doi:10.1016/j.cell.2012.10.039 (2012).

68 Patterson, M. *et al.* Microinjection of galanin-like peptide into the medial preoptic area stimulates food intake in adult male rats. *Journal of neuroendocrinology* **18**, 742-747, doi:10.1111/j.1365-2826.2006.01473.x (2006).

69 Henry, H. L. & Norman, A. W. *Encyclopedia of hormones*. (Academic Press, 2003).

70 Takenoya, F. *et al.* Neuronal interactions between galanin-like-peptide- and orexin- or melanin-concentrating hormone-containing neurons. *Regulatory peptides* **126**, 79-83, doi:10.1016/j.regpep.2004.10.004 (2005).

71 Kageyama, H. *et al.* Galanin-like peptide promotes feeding behaviour via activation of orexinergic neurones in the rat lateral hypothalamus. *Journal of neuroendocrinology* **18**, 33-41, doi:10.1111/j.1365-2826.2005.01382.x (2006).

72 Reaux-Le Goazigo, A. *et al.* Apelin and the proopiomelanocortin system: a new regulatory pathway of hypothalamic alpha-MSH release. *American journal of physiology. Endocrinology and metabolism* **301**, E955-966, doi:10.1152/ajpendo.00090.2011 (2011).

73 Lv, S. Y. *et al.* Central apelin-13 inhibits food intake via the CRF receptor in mice. *Peptides* **33**, 132-138, doi:10.1016/j.peptides.2011.11.011 (2012).

74 Sunter, D., Hewson, A. K. & Dickson, S. L. Intracerebroventricular injection of apelin-13 reduces food intake in the rat. *Neuroscience letters* **353**, 1-4, doi:10.1016/s0304-3940(03)00351-3 (2003).

75 O'Shea, M., Hansen, M. J., Tatemoto, K. & Morris, M. J. Inhibitory effect of apelin-12 on nocturnal food intake in the rat. *Nutritional neuroscience* **6**, 163-167, doi:10.1080/1028415031000111273 (2003).

76 Bloom, F. E., Battenberg, E. L., Rivier, J. & Vale, W. Corticotropin releasing factor (CRF): immunoreactive neurones and fibers in rat hypothalamus. *Regulatory peptides* **4**, 43-48, doi:10.1016/0167-0115(82)90107-0 (1982).

77 Paull, W. K. *et al.* Immunocytochemical localization of CRF in the ovine hypothalamus. *Peptides* **3**, 183-191, doi:10.1016/0196-9781(82)90049-3 (1982).

78 Reaux, A., Gallatz, K., Palkovits, M. & Llorens-Cortes, C. Distribution of apelin-synthesizing neurons in the adult rat brain. *Neuroscience* **113**, 653-662, doi:10.1016/s0306-4522(02)00192-6 (2002).

79 McAllen, R. M., Tanaka, M., Ootsuka, Y. & McKinley, M. J. Multiple thermoregulatory effectors with independent central controls. *European journal of applied physiology* **109**, 27-33, doi:10.1007/s00421-009-1295-z (2010).

80 Wang, L., Tian, Y., Kim, J. & Yin, H. The key local segments of human body for personalized heating and cooling. *J Therm Biol* **81**, 118-127, doi:10.1016/j.jtherbio.2019.02.013 (2019).

81 Romanovsky, A. A. Thermoregulation: some concepts have changed. Functional architecture of the thermoregulatory system. *American journal of physiology. Regulatory, integrative and comparative physiology* **292**, R37-46, doi:10.1152/ajpregu.00668.2006 (2007).

82 Rolls, E. T., Grabenhorst, F. & Parris, B. A. Warm pleasant feelings in the brain. *NeuroImage* **41**, 1504-1513, doi:10.1016/j.neuroimage.2008.03.005 (2008).

83 Johnson, J. M., Minson, C. T. & Kellogg, D. L., Jr. Cutaneous vasodilator and vasoconstrictor mechanisms in temperature regulation. *Comprehensive Physiology* **4**, 33-89, doi:10.1002/cphy.c130015 (2014).

84 Mundel, T., Bunn, S. J., Hooper, P. L. & Jones, D. A. The effects of face cooling during hyperthermic exercise in man: evidence for an integrated thermal, neuroendocrine and behavioural response. *Experimental physiology* **92**, 187-195, doi:10.1113/expphysiol.2006.034934 (2007).

85 Simmons, S. E., Mundel, T. & Jones, D. A. The effects of passive heating and head-cooling on perception of exercise in the heat. *European journal of applied physiology* **104**, 281-288, doi:10.1007/s00421-007-0652-z (2008).

86 Conceicao, E. P. S., Madden, C. J. & Morrison, S. F. Neurons in the rat ventral lateral preoptic area are essential for the warm-evoked inhibition of brown adipose tissue and shivering thermogenesis. *Acta physiologica (Oxford, England)* **225**, e13213, doi:10.1111/apha.13213 (2019).

87 Harding, E. C. *et al.* A Neuronal Hub Binding Sleep Initiation and Body Cooling in Response to a Warm External Stimulus. *Current biology : CB* **28**, 2263-2273 e2264, doi:10.1016/j.cub.2018.05.054 (2018).

88 Picelli, S. *et al.* Full-length RNA-seq from single cells using Smart-seq2. *Nature protocols* **9**, 171-181, doi:10.1038/nprot.2014.006 (2014).

Figures

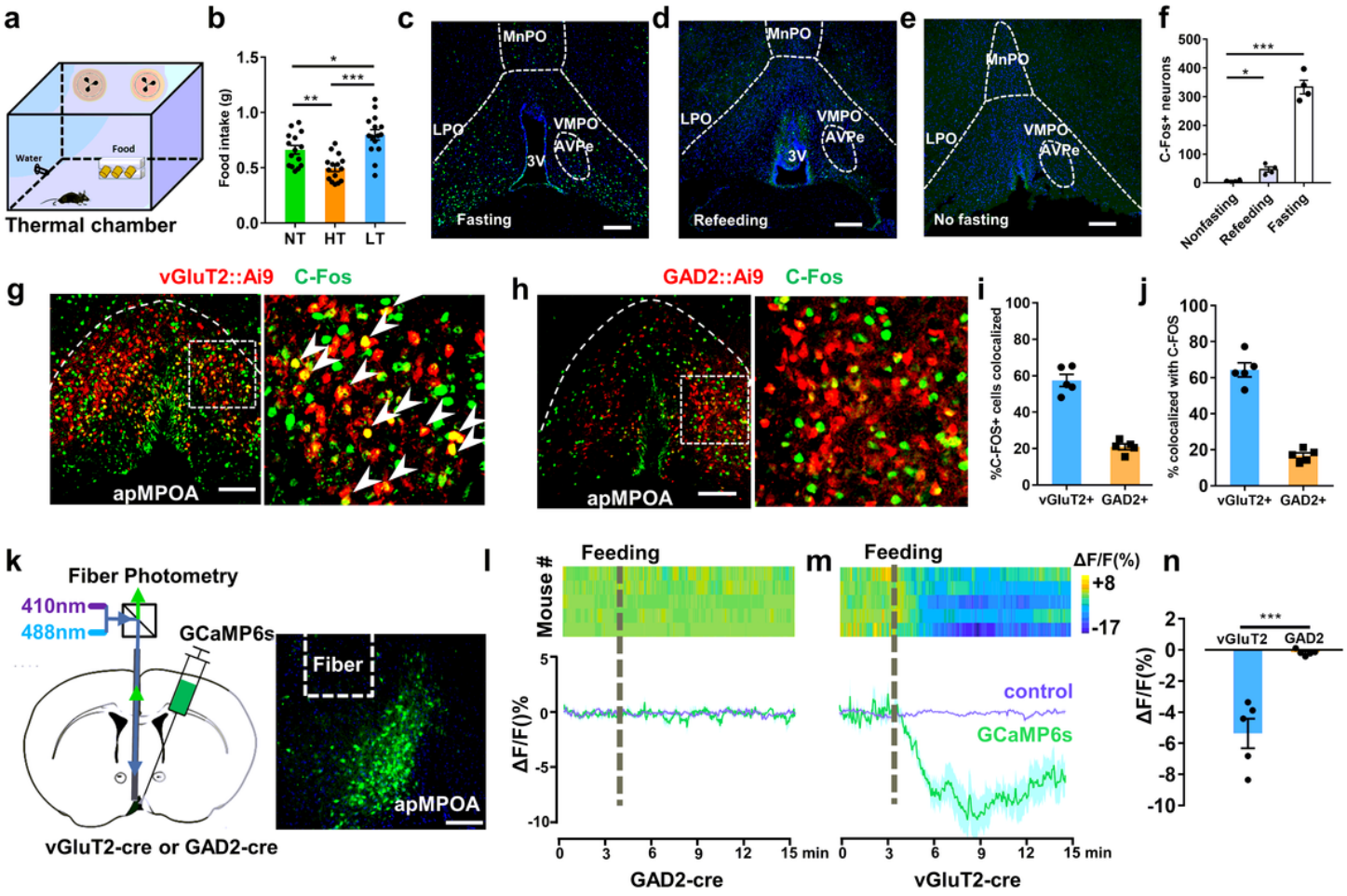

Figure 1

Glutamatergic apMPOA neurons respond to altered dietary states a, Scheme of feeding test in a temperature-controlled chamber. b, Differences of 2-hour food intake among the three ambient temperatures. NT, neutral temperature; HT, high temperature; LT, low temperature. One-way ANOVA and post hoc least significant difference (LSD) multiple comparison, *p < 0.05, ** p < 0.01, ***p < 0.001, n = 15

animals for each group. c-f, C-Fos expressions in the apMPOA in three dietary states: 12-hour fasting, 2-hour refeeding and nonfasting. AVPe, anteroventral periventricular nucleus; VMPO, ventromedial preoptic nucleus; MnPO, median preoptic nucleus; 3V, the 3rd ventricle. Scale bar, 100 μm. One-way ANOVA and post hoc LSD multiple comparison, *p < 0.05, ***p < 0.001, n = 4 animals for each group. g-h, Colocalizations of fasting-induced C-Fos (green) with vGluT2+ (red) and GAD2+ neurons (red) in vGluT2::Ai9 (G) and GAD2::Ai9 mice (H) . Images were obtained from transgenic mice by crossing Ai9 (Cre-dependent tdTomato reporter) with vGluT2-cre (G), and Ai9 with GAD2-cre (H). Scale bar, 100 μm. i, Percentage of C-Fos+ neurons that are vGluT2+ and GAD2+. n = 5 animals for each group. j, Percentage of vGluT2+ and GAD2+ neurons that express C-Fos. n = 5 animals for each group. k, Scheme of fiber photometry setup, and representative coronal section of apMPOA neurons expressing GCaMP6s. Scale bar, 100 μm. l-m, GcaMP6s (mean, green line; SEM, green shading) and control (mean, purple line; SEM, purple shading) signal changes (ΔF/F) in response to feeding in GAD2-cre (l) and vGluT2-cre mice (m) after 24-hour fasting. n = 5 animals for each group. n, The mean ΔF/F in a 5-minute window after the onset of feeding. T test, ***p < 0.001, n = 5 animals for each group.

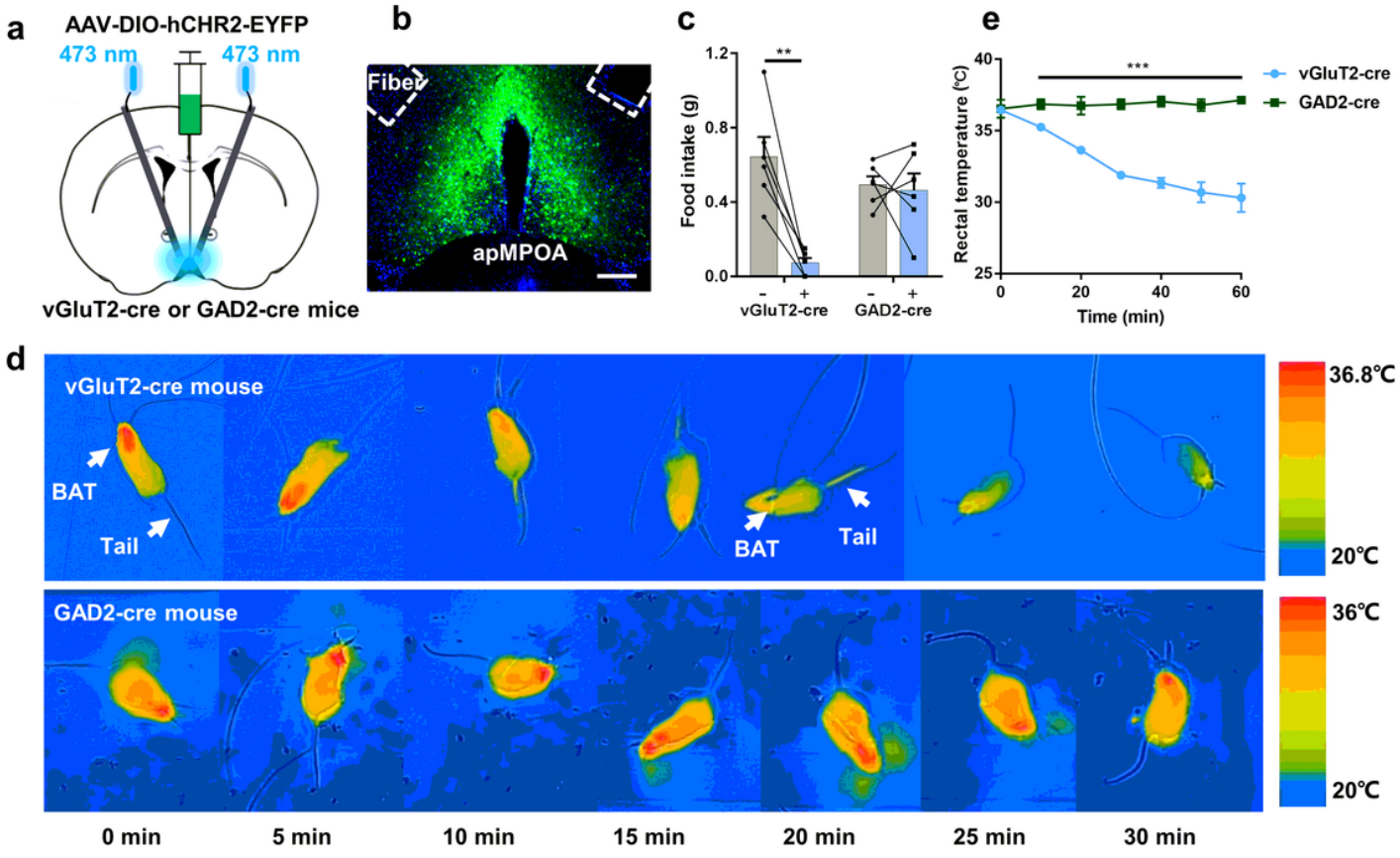

Figure 2

Opto-stimulation on glutamatergic apMPOA neurons induces decreases in food intake and rectal temperature a-b, Schematic and representative coronal images of injecting AAV virus expressing ChR2 into the apMPOA in vGluT2-cre and GAD2-cre mice and oblique optical fiber implantation above the apMPOA. Scale bar, 100 μm. c, Opto-stimulation (2 hours) on the apMPOA neurons in vGluT2-cre mice

decreased food intake, but not in GAD2-cre mice. Paired t tests, **p < 0.01, n = 6 animals for each group. d, Infrared thermography revealed that opto-stimulation (30 min) on the apMPOA neurons in vGluT2-cre mice, but not GAD2-cre mice, promoted tail heat dissipation and inhibited BAT thermogenesis. e, Opto-stimulation (60 min) on the apMPOA neurons in vGluT2-cre mice induced transient rectal temperature decrease, but not in GAD2-cre mice. Two-way repeated-measure ANOVA, ***p<0.001, n = 6 animals for each group.

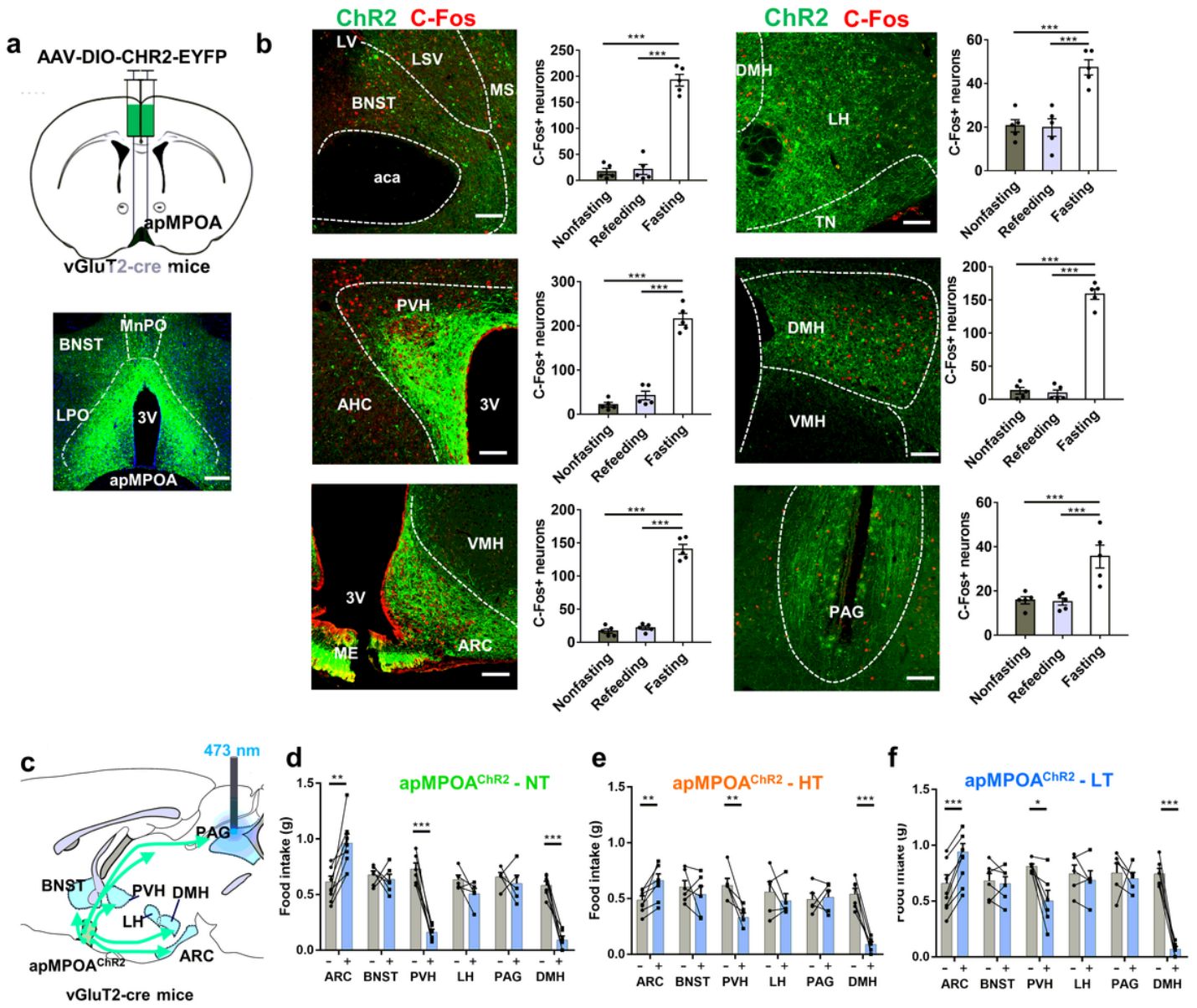

Figure 3

Optogenetic terminal activations on the ARC and PVH orchestrate food intake a, Schematic and representative coronal images of injecting AAV virus expressing ChR2 into the apMPOA in vGluT2-cre mice. Scale bar, 100 μm. b, Representative images of downstream targets of glutamatergic apMPOA neurons (green, ChR2), including BNST, LH, PVH, DMH, ARC and PAG, in which fasting-induced C-Fos expression can be clearly observed compared to the re-feeding and nonfasting groups (red, C-Fos). Scale

bar, 100 μm. One-way ANOVA and post hoc LSD multiple comparison, ***p < 0.001, n = 5 animals for fasting, nonfasting and refeeding groups. c, Schematic sagittal image of terminal activation on individual target (PAG shown here), which allows for selective activation on the downstream target of apMPOA. d-f, Two-hour food intake with (+, blue boxes) and without (-, gray boxes) opto-stimulation on the target regions during ambient temperatures. Paired t tests, *p < 0.05, **p < 0.01, ***p < 0.001.

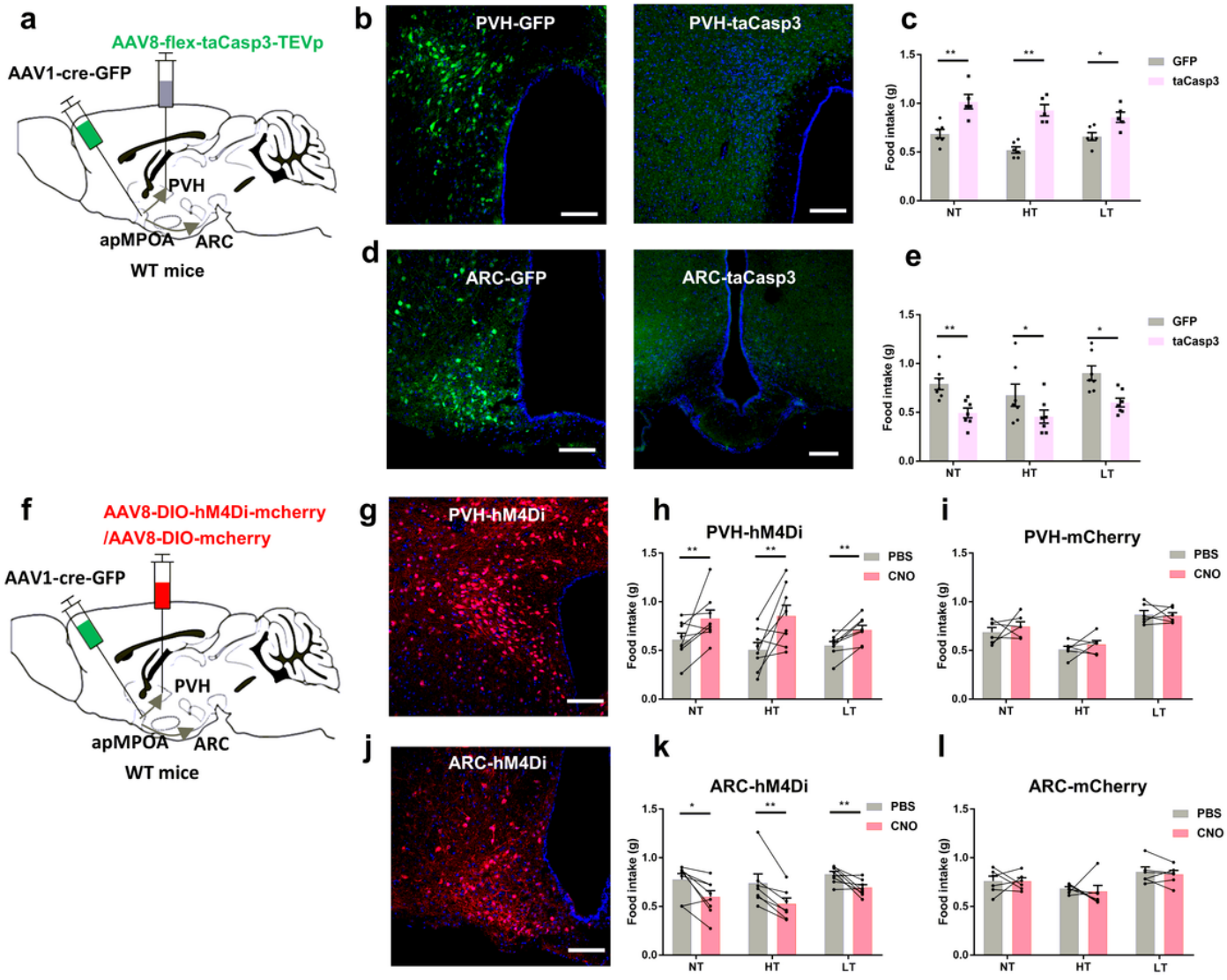

Figure 4

Genetic ablation and chemogenetic inhibition on the postsynaptic apMPOA-recipient neurons in ARC/PVH reversely modulate feeding behavior a, Schematic image showing genetic ablation of apMPOA-recipient neurons in ARC/PVH individually (PVH shown here) in wild type mice by injecting anterograde transsynaptic AAV1-Cre-GFP in apMPOA that will encodes Cre recombinase and GFP in the downstream postsynaptic neurons, and Cre-dependent caspase-3 in the ARC and PVH. b,d, Representative images showing preserved transsynaptic neurons in PVH (upper left image) and ARC (lower left image) that expressed GFP in the control group, but ablated transsynaptic neurons in the PVH (upper right image) and ARC (lower right image) in taCasp3-injected mice. Scale bar, 100 μm. c, The ablation of transsynaptic

neurons in the PVH significantly increased food intake compared to that in the controls in all thermal conditions. Two-way repeated-measure ANOVA and post hoc LSD multiple comparison, *p<0.05, **p<0.01, n = 5 animals in the taCasp3 group and n =6 animals in the control group. e, The ablation of transsynaptic neurons in the ARC significantly decreased food intake compared to that in the controls in all thermal conditions. Two-way repeated-measure ANOVA and post hoc LSD multiple comparison, *p<0.05, **p<0.01, n = 7 animals in the taCasp3 and control groups. f, Schematic image showing the chemogenetic inhibition of apMPOA-recipient neurons in ARC/PVH individually (PVH shown here) in wild type mice by injecting anterograde transsynaptic AAV1-Cre-GFP in apMPOA that will encodes Cre recombinase and GFP in the downstream postsynaptic neurons, and Cre-dependent DREAD-Gi in the ARC and PVH. g, j, Representative images show that transsynaptic neurons in the PVH (g) and ARC (j) expressed hM4Di-mCherry (GFP in green channel was not shown). Scale bar, 100 μm. h, The chemogenetic inhibition of postsynaptic neurons in the PVH significantly increased food intake after intraperitoneal injection of CNO under all thermal conditions compared to controlled PBS injection. Two-way repeated-measure ANOVA and post hoc LSD multiple comparison, **p<0.01, n = 8 animals. k, The inhibition of neurons in the ARC significantly decreased food intake. Two-way repeated-measure ANOVA and post hoc LSD multiple comparison, *p<0.05, **p<0.01, n = 8 animals, one mouse in HT condition was excluded due to incomplete data. i, l, The controlled groups that expressed mCherry in PVH (i) and ARC (l) did not show food intake changes between CNO and PBS injections. Two-way repeated-measure ANOVA and post hoc LSD multiple comparison, n = 6 animals in both PVH-mCherry and ARC-mCherry groups.

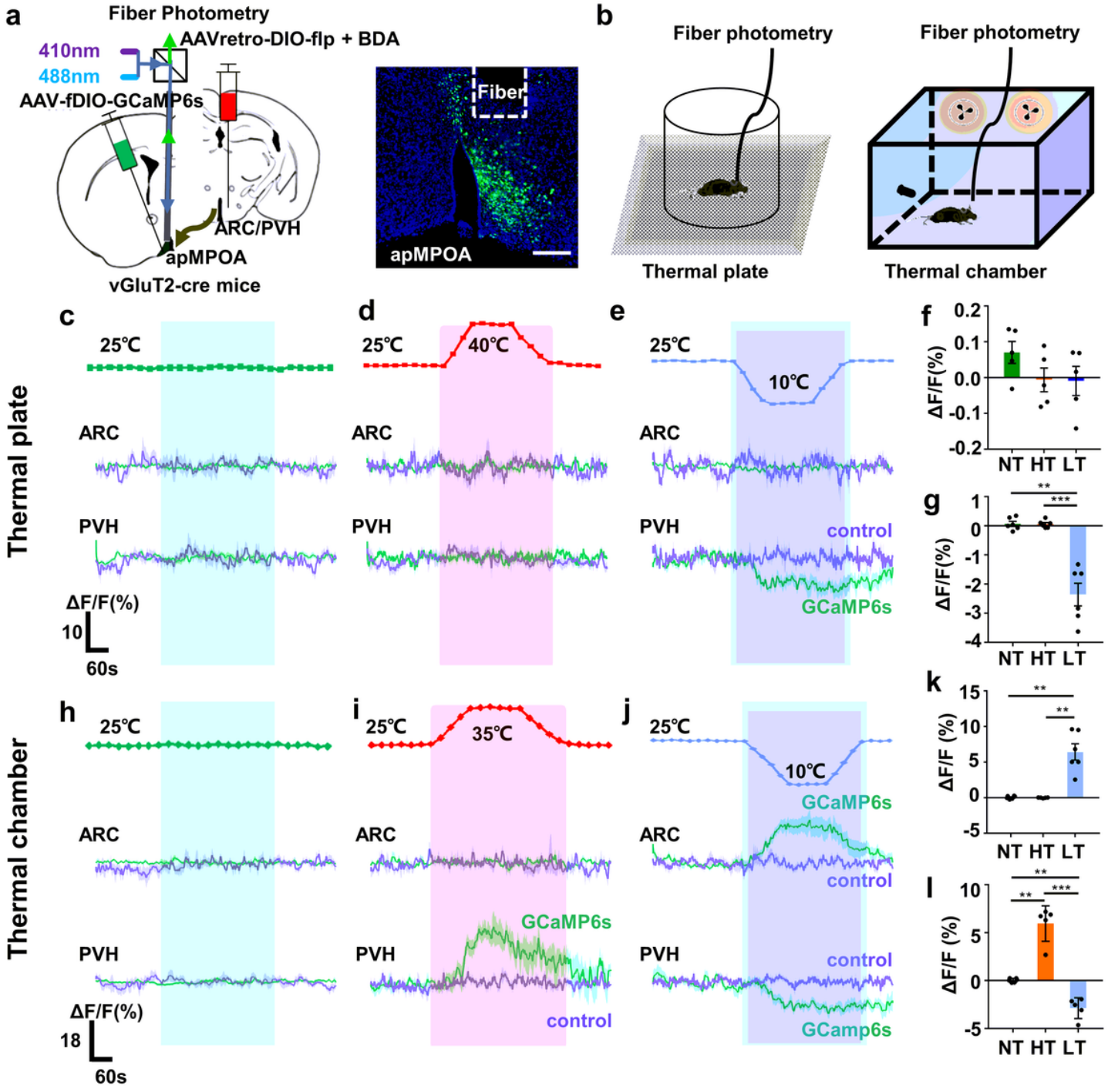

Figure 5

PVH and ARC-projecting apMPOA neurons are responsive to ambient thermal exposure, but not to local stimuli. a, Schematic and representative coronal images of AAVretro-DIO-flp virus injection (mixed with red fluorescent biotinylated dextran amines to indicate the injection range) into the PVH and ARC (ARC shown here) and AAV-fDIO-GCaMP6s into the apMPOA in vGluT2-cre mice. The optical fiber was placed 200 μm above the apMPOA neurons. BDA, biotinylated dextran amines. Scale bar, 100 μm. b, Schematic of thermal exposure by temperature-controlled plate and chamber. c-e, GcaMP6s (mean, green line; SEM,

green shading) and control (mean, purple line; SEM, purple shading) signal changes (ΔF/F%) of the ARC (top) and PVH-projecting (bottom) apMPOA neurons in response to local thermal stimuli: neutral (25°C, green dotted line in Fig. 5c), hot (25°C→40°C, red dotted line in Fig. 5d), cold (25°C→10°C, blue dotted line in Fig. 5e). h-j, GcaMP6s and control signal changes (ΔF/F%) of the ARC (top) and PVH-projecting (bottom) apMPOA neurons in response to ambient thermal exposure: neutral (25°C, green dotted line in Fig. 5h), hot (25°C→35°C, red dotted line in Fig. 5i), cold (25°C→10°C, blue dotted line in Fig. 5j). f, g, k, l, Bar graphs show mean ΔF/F response of ARC (thermal plate: f, thermal chamber: k) and PVH-projecting (thermal plate: g, thermal chamber: l) apMPOA neurons in a 5-minute window after the onset of thermal exposure. One-way repeated-measure ANOVA and post hoc LSD multiple comparison, **p<0.01, ***p<0.001. N=6 for both PVH and ARC groups, but n = 5 animals were included into statistical ANOVA in ARC groups in cold plate and hot chamber, PVH group in cold chamber and hot chamber due to incomplete data.

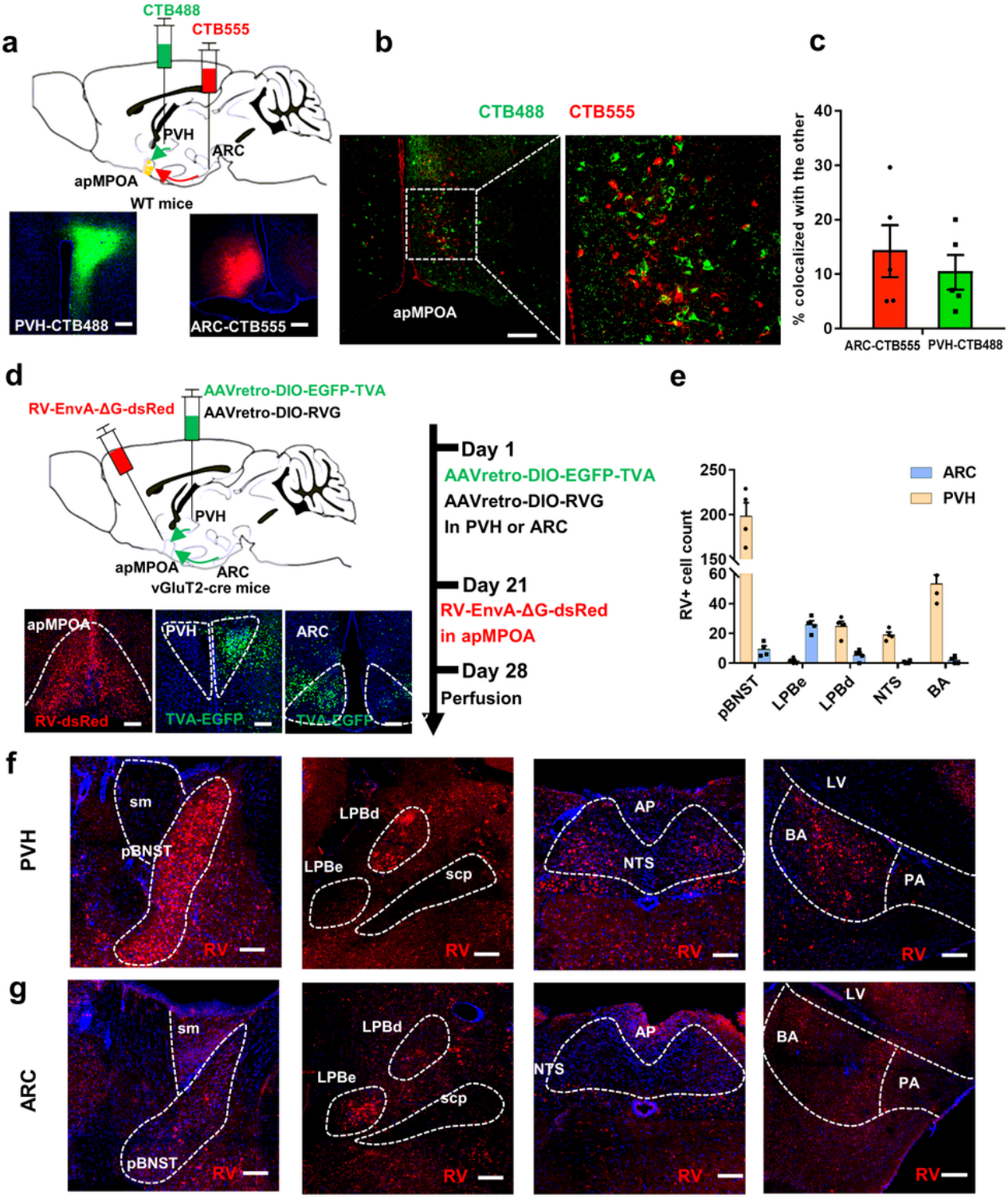

Figure 6

Retrograde labeling for the two subsets of anatomically differentiated PVH and ARC-projecting apMPOA neurons a, Schematic and representative coronal images of the injection of CTB 488 and CTB 555 into PVH and ARC of wild type mice respectively. Scale bar, 100 μm. b-c, Colocalizations of retrograde-labeled neurons in the apMPOA from the PVH (green) and ARC (red), n = 5 animals for both groups. Scale bar, 100 μm. d, Schematic and representative coronal images of the injection of Cre-dependent AAVretro

vector expressing RV helpers into the PVH or ARC on day 1 and RV-EnvA-ΔG-dsRed on day 21 into the apMPOA of vGluT2-cre mice. Scale bar, 100 μm. e, Quantification of numbers of retrogradely labeled cells in different regions in ipsilateral sides of the injected apMPOA. n = 4 animals for both groups. f, Typical coronal images of DsRed-expressing neurons in posterior part of the BNST (pBNST), LPBd, NTS and BA in the group with RV helpers-injection into the PVH. Scale bar, 100 μm. g, Typical coronal images of DsRed-expressing neurons in LPBe, but sparse neurons in the pBNST, NTS and BA in the group with RV helpers-injection into the ARC. Scale bar, 100 μm.

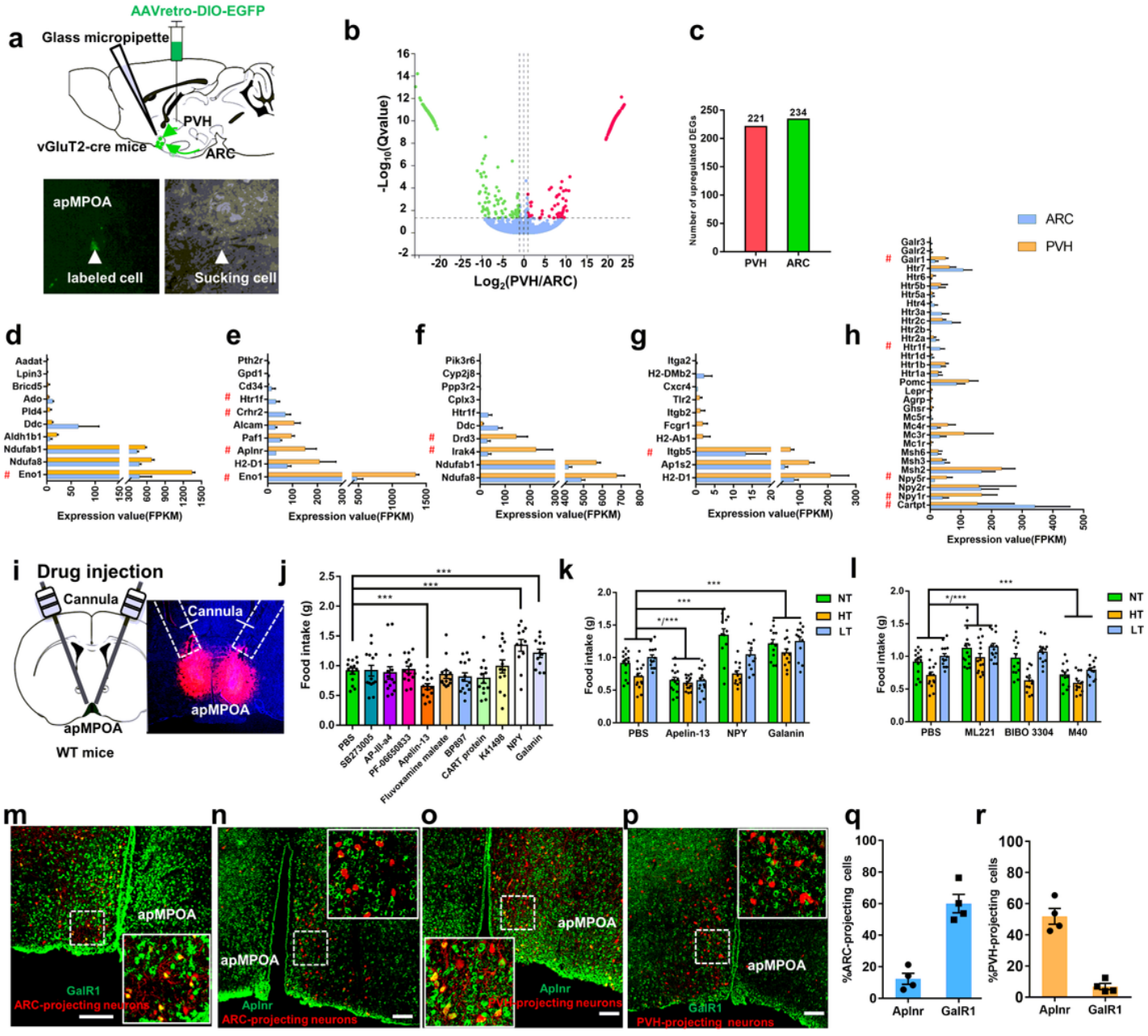

Figure 7

Molecular markers for the PVH and ARC-projecting apMPOA neurons a, Schematic image of the injection of Cre-dependent AAVretro-GFP into PVH or ARC of vGluT2-cre mice, and representative retrograde GFP-

labeled cell body sucked by a glass micropipette. b-c, Volcano plot and bar graph depicting the comparison of transcript abundance between PVH and ARC-projecting apMPOA neurons. Genes upregulated in PVH-projecting apMPOA neurons are indicated in red, whereas those in ARC-projecting apMPOA neurons are indicated in green. d-g, The expression (FPKM) of DEGs in the KEGG pathway categories: metabolism (d), environmental information processing (e), organismal systems (f), cellular processes (g). The candidate marker genes are indicated in red #. h, The expression of genes related to feeding peptides and receptors. The candidate marker genes are indicated in red #. i, Schematic and representative coronal images of cannula injection of antagonists or agonists of the candidate genes. j, Feeding test after cannula injection of antagonists or agonists of the selected candidate genes during normothermia shows that apelin, galanin and NPY injections cause food intake changes. One-way repeated-measure ANOVA and post hoc LSD multiple comparison, ***p<0.001. k, Feeding test after apelin, galanin and NPY injections at ambient temperatures. Compared with PBS injection, apelin-13 robustly suppressed food intake at ambient temperatures. The galanin robustly promoted food intake at ambient temperatures. NPY only promoted food intake during normothermia, but not during high or low temperature. Two-way repeated-measure ANOVA and post hoc LSD multiple comparison, *p<0.05, ***p<0.001. l, Feeding test after the injections of apelin, galanin and NPY receptors antagonists at ambient temperatures. Compared with PBS injection, ML221 (apelin receptor antagonist) and M40 (GalR1 antagonist) reversed the food intake by the agonists. Blocking the NPY receptor (BIBO 3304) did not induce food intake changes. Two-way repeated-measure ANOVA and post hoc LSD multiple comparison, *p<0.05, ***p<0.001. m, Colocalizations of ARC-projecting apMPOA neurons (red) with GalR1+ neurons (green) in vGluT2-Cre mice. GalR1, galanin receptor 1. Scale bar, 100 μm. n, Colocalizations of ARC-projecting apMPOA neurons (red) with Aplnr+ neurons (green) in vGluT2-Cre mice. Aplnr, apelin receptor. Scale bar, 100 μm. o, Colocalizations of PVH-projecting apMPOA neurons (red) with Aplnr+ neurons (green) in vGluT2-Cre mice. Aplnr, apelin receptor. Scale bar, 100 μm. p, Colocalizations of PVH-projecting apMPOA neurons (red) with GalR1+ neurons (green) in vGluT2-Cre mice. GalR1, galanin receptor 1. Scale bar, 100 μm. q, Percentage of ARC-projecting apMPOA neurons that are GalR1+ and Aplnr+. n = 4 animals for each group. r, Percentage of PVH-projecting apMPOA neurons that are GalR1+ and Aplnr+. n = 4 animals for each group.

Supplementary Files

This is a list of supplementary files associated with this preprint. Click to download.

- MovieS1.mp4
- MovieS2.mp4
- MovieS3.mp4
- MovieS4.mp4
- FigureS1.tif
- FigureS2.tif

- FigureS3.tif
- FigureS4.tif
- FigureS5.tif
- FigureS6.tif
- FigureS7.tif
- SupplementaryFigureLegends.docx